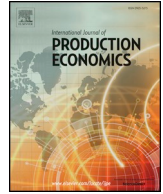




ELSEVIER

Contents lists available at ScienceDirect

International Journal of Production Economics

journal homepage: www.elsevier.com/locate/ijpe

A stochastic programming approach for electric vehicle charging station expansion plans

Mohannad Kabli^{a,*}, Md Abdul Quddus^a, Sarah G. Nurre^b, Mohammad Marufuzzaman^a, John M. Usher^a

^a Department of Industrial and Systems Engineering, Mississippi State University, Starkville, MS, 39759-9542, USA

^b Department of Industrial Engineering, University of Arkansas, AR, 72701, USA

ARTICLE INFO

Keywords:

Transportation
Electric vehicles
Charging station
Sample average approximation
Progressive hedging

ABSTRACT

The projected and current adoption rates of electric vehicles are increasing. Electric vehicles need to be recharged continually over time, and the energy required to ensure that is immense and growing. Given that existing infrastructure is insufficient to supply the projected energy needs, models are necessary to help decision makers plan for how to best expand the power grid to meet this need. A successful power grid expansion is one that enables charging stations to service the electric vehicle community. Thus, plans for power expansion need to be coordinated between the power grid and charging station investors. In this paper, we present a two-stage stochastic programming approach that can be used to determine a power grid expansion plan that supports the energy needs, or load, from an uncertain set of electric vehicles geographically dispersed over a region. The first stage determines where to expand the power grid, and the second stage determines where to locate charging stations. The key link between the first and second stage decisions is that charging stations can only be located in areas with sufficient power supply enabled by an expanded power grid. To solve the model, we utilize a hybrid approach that combines Sample Average Approximation and an enhanced Progressive Hedging algorithm. We enhance the Progressive hedging algorithm by applying rolling horizon and variable fixing techniques. To validate the proposed model and gain key insights, we perform computational experiments using realistic data representing the Washington, DC area. Our computational results indicate the robustness of the proposed algorithm while providing a number of managerial insights to the decision makers.

1. Introduction

The increase in electric vehicles' use by consumers and commercial businesses is shaping the future for a cleaner and more energy-efficient transportation system. The growth in adoption rates of electric vehicles is motivated by many reasons. First, advances in battery storage, allowing a Tesla model S to travel almost 300 miles (Tesla Model available, 2016) with a single charge, allows users to overcome the problem of range anxiety (Rezvani et al., 2015). Additionally, the U.S. government has many initiatives to encourage the adoption of electric vehicles. For example, in January 2014 U.S. Energy Secretary Ernest Moniz allocated \$50 million dollars for research on electric vehicles in support of the *Electric Vehicle Everywhere Grand Challenge* which aims to produce electric vehicles that are as affordable and convenient as internal combustion vehicles by 2022 (U.S. Department of Energy, 2014).

While the increase in the adoption of electric vehicles allows for the

transportation system to become less reliant on scarce and harmful fossil fuels, there are logistics considerations that need to be addressed as more electric vehicles become prevalent. Internal combustion engines require fuel to run, whereas electric vehicles require power from a battery. When an electric vehicle battery nears depletion, users commonly recharge at an electric vehicle charging station. As more electric vehicles take to the road, the charging station system needs to be expanded. Electric vehicle charging stations require sufficient energy, supplied from the power grid, to operate and recharge electric vehicle batteries. In order to support the expansion and new installation of electric vehicle charging stations, the power company needs to ensure they have sufficient energy flowing through their grid to meet the increased demand from these stations. Many power grids do not have sufficient supply to meet the projected increase in demand from electric vehicle charging stations (Yunus et al., 2011), and thus, power expansion plans need to be implemented. A recent study from Washington

* Corresponding author.

E-mail addresses: mrk297@msstate.edu (M. Kabli), mq90@msstate.edu (M.A. Quddus), snurre@uark.edu (S.G. Nurre), maruf@ise.msstate.edu (M. Marufuzzaman), usher@ise.msstate.edu (J.M. Usher).

<https://doi.org/10.1016/j.ijpe.2019.07.034>

Received 24 October 2018; Received in revised form 17 May 2019; Accepted 27 July 2019

0925-5273/ © 2019 Elsevier B.V. All rights reserved.

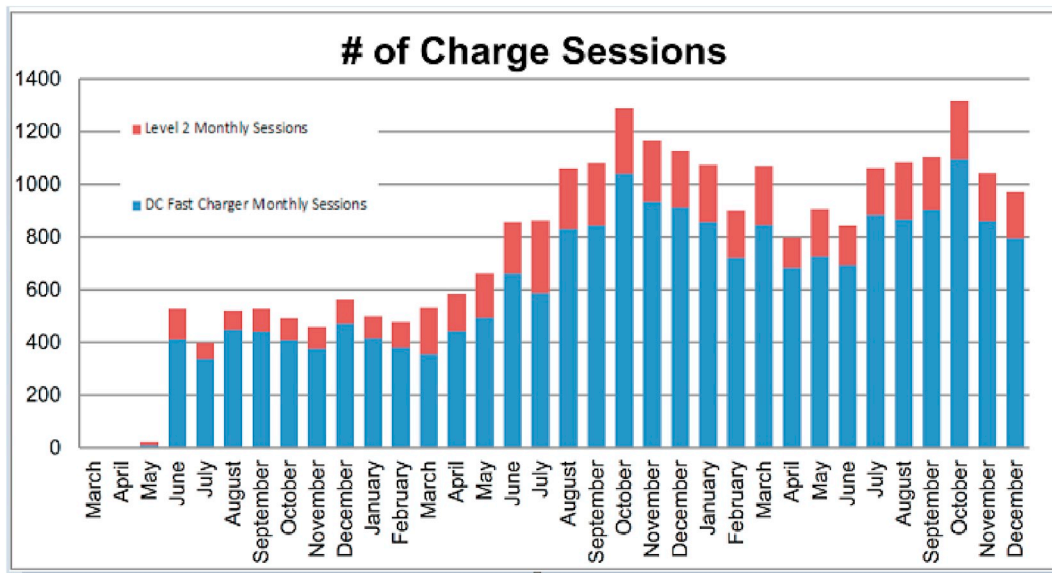


Fig. 1. Number of charging sessions monthly for the period 2012–2015 (Washington State Department of Transportation, 2015).

State's Department of Transportation reveals that a total of 228,725 kWh of energy were supplied to charge electric cars between 2012 and 2015, which is equivalent to displacing 22,397 gallons of gas (Washington State Department of Transportation, 2015). Moreover, since the stations were first opened in 2012, they have been used a total of 25,888 times as of December 2015, as shown in Fig. 1. It is expected that the load from electric vehicles in the state of Washington will reach 107 MW by 2029 (City Light, 2010). Hence, the power company needs to be prepared in advance to handle these additional power requirements.

Expanding the power grid takes time, requiring that the power company make decisions based on uncertain aggregate projections on the adoption rate of electric vehicles per year by geographic region. This uncertainty in adoption rates translates into uncertainty in predicting the demand for electric vehicle charging by location. Thus, the power company must work with this uncertainty as they decide where to expand the power grid to support the installation of charging stations over time.

To address this need, this study develops a two-stage stochastic programming model where the first stage determines the power expansion plan for a geographic region that is projected to experience electric vehicle growth. Specifically, we model locations within a power grid and determine whether or not to expand the power capabilities at each discrete power location. To inform this first stage decision, we consider a set of candidate locations where charging stations can be installed, the necessary supporting power capabilities by vehicle location, and an aggregated projection for the flow, or demand, for each charging location per year. Once the power expansion plan is decided in the first stage, we then examine each candidate location to determine whether a charging station should be installed and its size. The key link between the first and second stage decisions is that charging stations can only be installed in locations with sufficient power supply, or equivalently, where the power grid has been expanded. The goal of this model is to maximize the total profit from expanding the power grid and locating charging stations.

Until now a number of researchers have studied the problem of locating electric vehicle charging stations under deterministic settings. Ip et al. (2010) use a clustering approach of electric vehicle charging demand in an urban setting to inform the location plans for the battery-driven electric vehicle charging stations. Chen and Kockelman (2013) perform regression analysis on parking survey data to determine where to locate charging stations in parking locations. Using a flow-based set

covering model, Wang and Lin (2009) determine the optimal locations for the electric vehicle charging stations. Frade et al. (Ribeiro and Gonçalves, 2011) use a maximal covering model to determine where to locate electric vehicle charge stations within Lisbon, Portugal. MirHassani and Ebrazi (2012) reformulate a mixed integer linear programming model based on the flow refueling location model (FRLM) developed by Kuby and Lim (2005). The main idea of FRLM is to locate several charging stations along long round trips using maximum cover. Bouche et al. (Baouche et al., 2014) used realistic trip based origin-destination (OD) data to determine the energy consumption of the electric vehicles while identifying the optimal location of the charging stations by formulating an integer programming model. Most recently, Chung and Kwon (2015) use the FRLM as a foundation to locate electric vehicle charging stations under a multi-time period planning model. The authors employ a forward myopic method and a backward myopic method to solve the multi-time period optimization model.

Alternatively, to generate a more reliable solution, a number of studies have developed stochastic models to locate electric vehicle charging stations. For instance, Pan et al. (2010) develop a two-stage stochastic program to optimally locate the stations prior to the realization of battery demands, loads, and generation capacity of renewable power sources. Ravichandran et al. (2016) propose a multi-time period mixed-linear integer programming model to determine an optimal control strategy for a charging station equipped with power storage, integrated EVs, and sources of renewable energies. The authors further propose a stochastic chance-constrained programming model that considers uncertainty in demand and power generation, EV state of charge, and the times of connection and disconnection. Xi et al. (2013) use a three-step combined simulation and optimization approach to determine where to locate electric vehicle charging stations as well as which charging level should be installed at each station. Mak et al. (2013) examine a robust optimization model that determines how to build the electric vehicle swapping station infrastructure given limited information regarding the electric vehicle adoption rates. Bayram et al. (2013) propose a stochastic model that determines how to operate an electric vehicle charge station efficiently through the use of an energy storage device under stochastic demand. Zhu et al. (2014) presents a dynamic optimization framework that considers multiple charging stations and cars charging at the same time. The key objective is to provide cars with the optimal charging rate that minimizes charging costs based on stochastic optimal control methods. Most recently, Hosseini and MirHassani (2015) introduce a two-stage stochastic

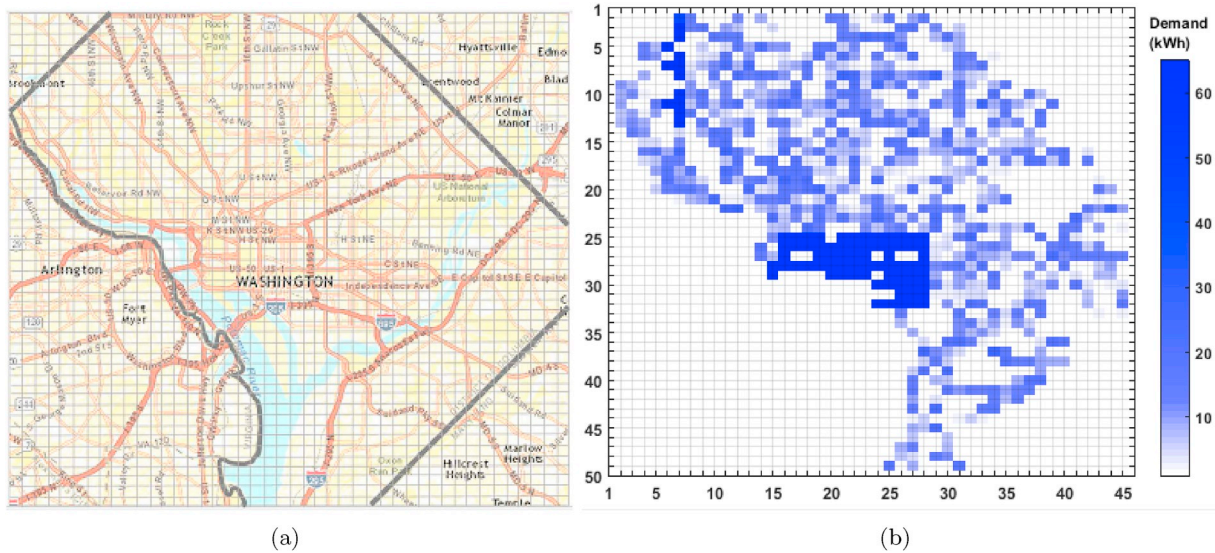


Fig. 2. Network representation (Original map obtained from (ArcashingtonA, 2016)) and geographical demand distribution of Washington DC.

Table 1
Different power expansion and charging station budget scenarios.

Scenarios		Yearly Budget (thousand \$)				
		2017	2018	2019	2020	2021
Base Case	B_i^e	5000	6000	7000	8000	9000
	B_i^c	400	550	700	850	1000
Scenario 1	B_i^e	5000	6000	7000	8000	9000
	B_i^c	600	825	1050	1275	1500
Scenario 2	B_i^e	7500	9500	10,500	12,000	13,500
	B_i^c	400	550	700	850	1000
Scenario 3	B_i^e	7500	9500	10,500	12,000	13,500
	B_i^c	600	825	1050	1275	1500

refueling station location model based on a finite number of scenarios that incorporate uncertainties of traffic flows. A two-step heuristic algorithm is used to solve the optimization problem where the first step reduces the size of the problem by solving a relaxed version of the original model while the second step applies a greedy algorithm to locate the charging stations.

Our model assumes that there is a collaboration between the power company and EV charging station decision makers. The reasons for making this assumption are twofold. First, the centralized decision making that we model shows a best-case scenario for such coordination. Second, we hope that although the power company and EV station decision-makers are likely to be privately run companies, given the government initiatives seeking to increase adoption of EVs that coordination between these two entities would be incentivized. The majority of research done in this regard assumes a centralized decision making, where all interested parties are assumed to work together. On the other side, few research has assumed a decentralized approach. Guo et al. (2016) assumes a competitive market, where charging stations' investors work toward maximizing their profits separately, and EV owners makes decisions on where to charge taking into consideration time and price issues. Yu et al. (Tong and Li, 2016) introduce a sequential game model between investors, aiming to maximize incomes, and the users, who are conflicted between owning a traditional gasoline-powered car or an EV.

By incorporating the realistic aspect that charging stations can be of different sizes, Ge et al. (2011) adopted a grid based partitioning approach to locate different sized charging stations in a given region. The authors used a genetic algorithm to locate charging stations in the grid

so that the users' loss on the way to the charging station can be minimized. Similarly, Jia et al. (2012) minimize the location cost of electric vehicle charging stations of different sizes under varying charging demands. Wang et al. (Wang and Lin, 2013) extend their previous work (Wang and Lin, 2009) by determining where to locate multiple types of electric vehicle recharging stations when considering application specifics such as budget, charging speed, and rerouting of electric vehicles based on charging station locations into account.

Another stream of research attempts to integrate both the power and transportation decisions under the same decision making framework. Wang et al. (2010) present a multi-objective planning model that considers a number of factors such as electric vehicles sustainable development, characteristics of charging station and consumers, distribution of the charging demand and the power grid. A solution algorithm is presented that considers demand priority and exploits the existing gas stations to locate charging stations. He et al. (2013) determine where to locate electric vehicle charging stations based on examining the interactions between the power and transportation networks. Specifically, the authors determine the equilibrium between electricity prices, traffic flow, and power flow which is utilized to determine the optimal location of the electric vehicle charging stations. The mathematical model is solved using an active-set decomposition algorithm. Sweda and Klabjan (2011) develop an agent-based decision support system to identify the patterns in residential electric vehicle ownership and driving activities to enable strategic deployment of new charging infrastructures. Galus and Andersson (2008) further use an agent-based approach and model the recharging behavior of large numbers of autonomous Plug-In Hybrid Electric Vehicles (PHEV) that allows sufficient support from the power grid via demand management using a nonlinear pricing model. Note that all the models discussed above attempt to locate charging stations by assuming that the key modeling parameters such as power demand, vehicle flow rate, charging capacity are known in advance and thus may produce unreliable or infeasible solutions when system uncertainties (e.g., technology, battery capacity, power demand, flow rate) are taken into consideration.

Another aspect, other than the charging stations location, that needs to be investigated is the consideration of electric power limitations when planning for EV. One paper by He et al. (2012) provides scheduling formulations that optimize the charging and discharging decisions and minimize the total cost. A global minimization scheduling aims to minimize the cost over a day for all EV, while a local minimization scheduling concentrates on optimizing some smaller region. The authors employed an interior point method to solve the proposed

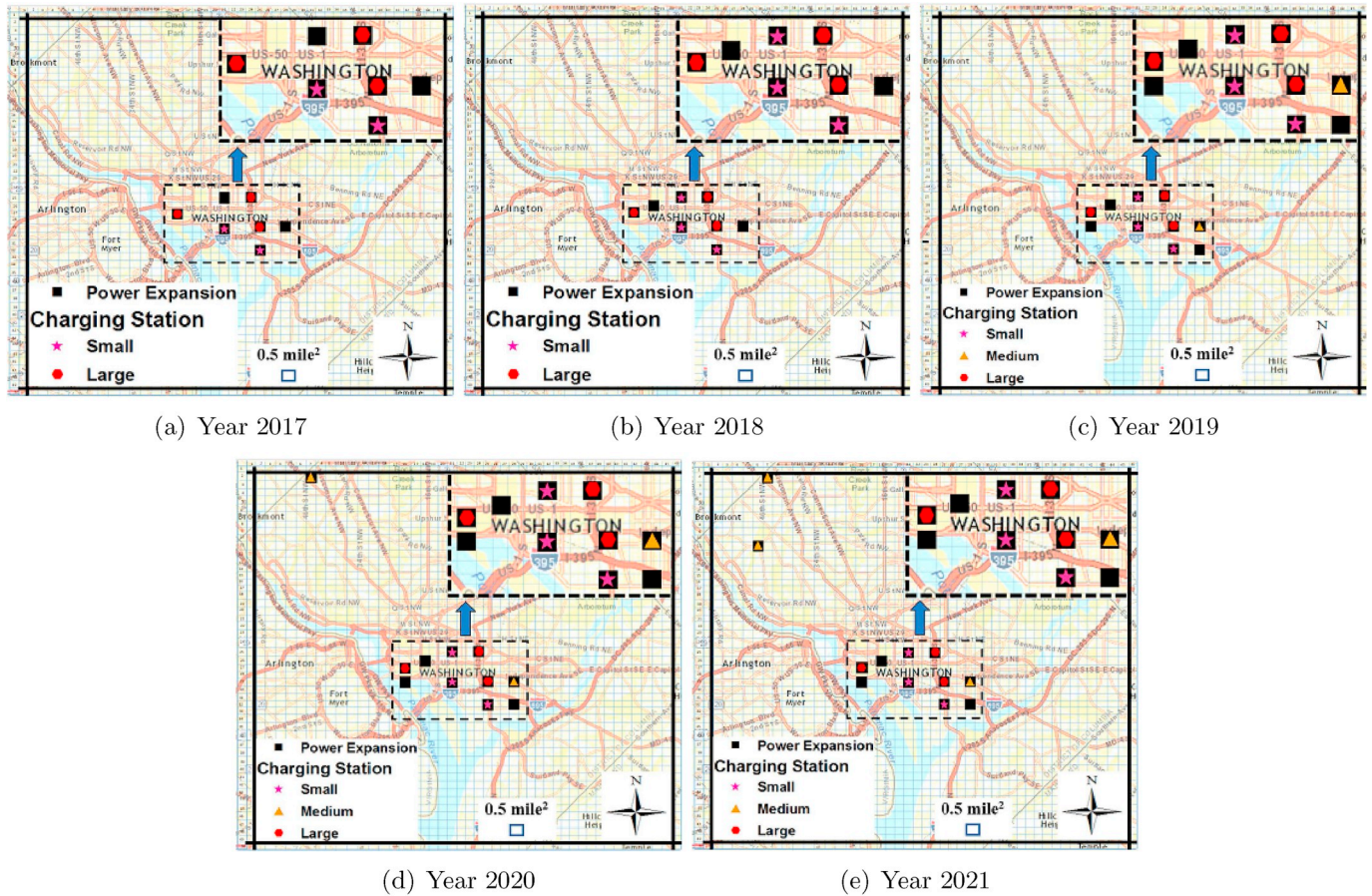


Fig. 3. Electric vehicle charging station expansion planning under base case scenario.

optimization model. Hajimiragha et al. (2010) aim to optimally utilize the electric grid during off-peak period to charge EVs using MIP. To better control the load from the charging EV cars on the grid, Richardson et al. (2012) develop a linear program that optimizes the rate at which EV charge to control the electric voltage and maximize the total power transferred to the cars within network limitations. Rotering and Ilic (2011) propose two dynamic programming algorithms that help in avoiding the overloading of the electric grid. The first one optimizes charging time to reduce electricity costs while the second one incorporates Vehicle-to-Grid (V2G) energy transfer to support the grid. Liu et al. (2015) presents different control methods (e.g., grid-to-vehicle and V2G) that balance the bidirectional communications between the EV and the power system. Rezai et al. (Akhavan-Rezai et al., 2015) study how parked EVs can be used as an energy storage device when plugged into the grid to respond to changes in demand. The authors employ a multi-stage model that schedules the charging session based on the pricing offers between an aggregator and the EV owners. Sundstrom and Binding (Sundstroem and Binding, 2012) consider the grid restrictions (e.g., voltage and power restrictions) in planning for the charging of electric vehicles. The aim is to control the load on the grid and provide each EV owner with a charging plan.

Note that none of the prior studies modeled the feasibility of locating electric vehicle charging stations based on power grid support. Moreover, there are very limited studies that consider system uncertainties (e.g., adoption rates, vehicle flow rate, charging capacity) that frequently impact the location and routing decisions of electric vehicles. To fill these gaps in the literature, this study develops a two-stage stochastic programming model that takes into account the uncertainty in both the adoption rates and charging behavior of

geographic regions. Further, we consider the important links between the power and transportation systems by ensuring that electric vehicle charging stations are only installed where there is sufficient power support. The model assumes a flow-based demand as opposed to a node-based demand, since it captures the dynamics of the transportation system. We solve the two-stage stochastic program using a hybrid decomposition algorithm comprised of Sample Average Approximation and an enhanced Progressive Hedging algorithm. The Progressive Hedging algorithm is enhanced through the application of rolling horizon and variable fixing techniques. From multiple numerical experiments, we show that the hybrid decomposition algorithm is capable of producing a near-optimum solution in a reasonable amount of time.

In addition to proposing the general model, another important contribution of this paper is applying this model to a real-world case study. We use Washington, DC as a testing ground in our case study. This region possesses a number of favorable factors (e.g., high income and dense population) that are likely to attract intensive electric vehicle infrastructure investment in the future.¹ For the problem modeled in this paper, the demand is not static but instead flows throughout a geographic region. We do not have access to real data representing the flow of EVs through the Washington, DC area. In absence of this data, we use the following rules and information to estimate the flow per cell, from which we generate the demand scenarios at each cell. First, we assume that flow is centered in the downtown area. We also know that there were 10,000 EVs in 2014 in Washington, DC (Washington State

¹ At present, there are over 700 public charging stations located in the DC and Baltimore area and this number is expected to increase in the coming future (Available from: <http://evadc.org/charging/>).

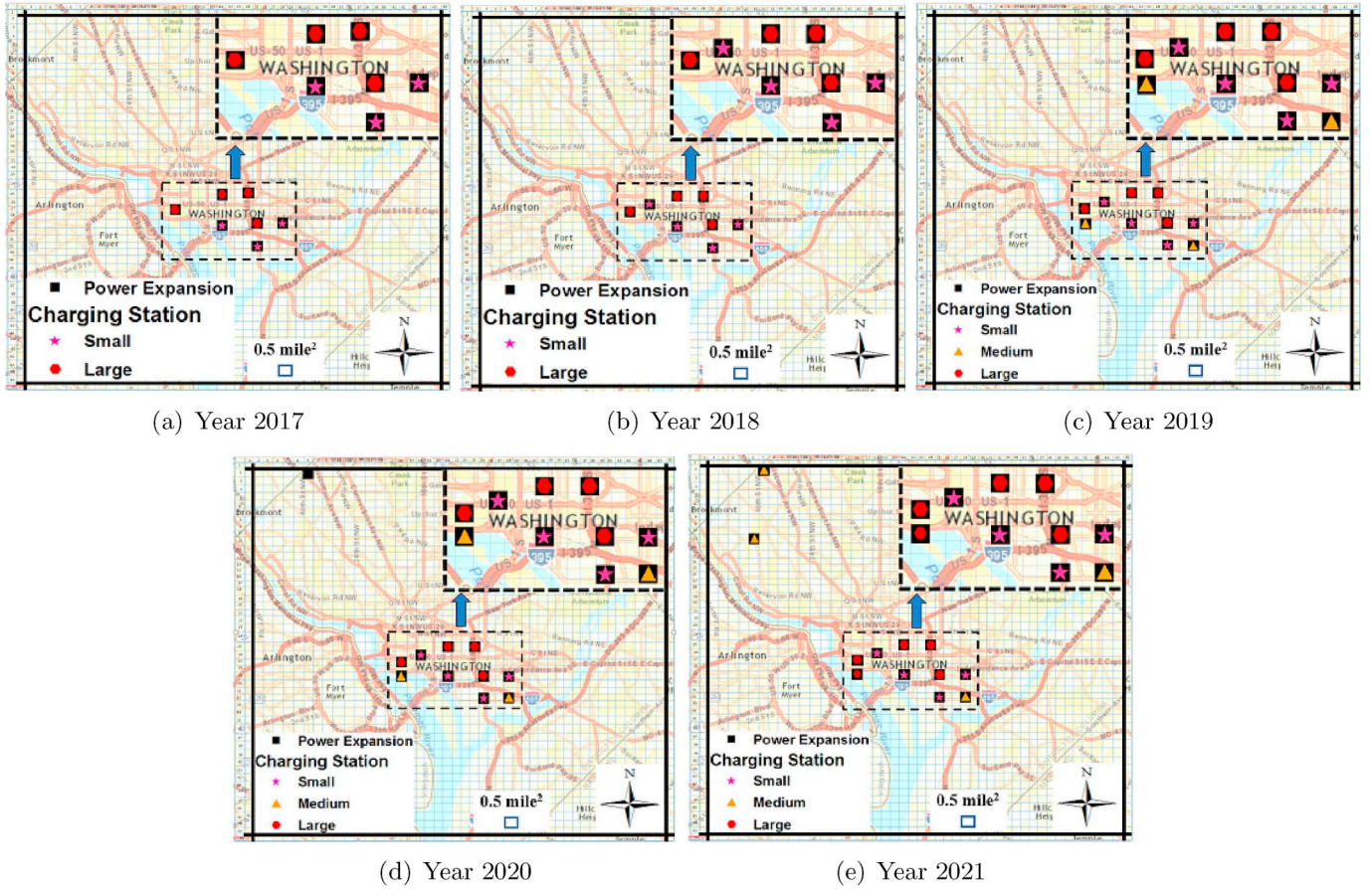


Fig. 4. Electric vehicle charging station expansion planning under scenario 1.

Department of Transportation, 2015). We determine which cells have and do not have a road passing through them, then we use balance of flow equally based on the degree at a particular location. For example, if the road forks, then flow is evenly split between each of the forks. If two roads join, the demand is summed from both directions. Using these rules and information, we carefully calculated the flow at each cell. In order to avoid double counting the satisfaction of flow demand, we imposed the rule that if a station is established in one cell, another station cannot be established in an adjacent cell. Demand scenarios has been generated based on the flow in each road. Different realizations have been proposed for each eligible cell by assuming that either flow will remain the same, increase, or decrease when the time comes for making the decision for locating a charging station. To account for the increase in demand over time, we multiplied the flow through each cell by a random factor between 1.0 and 2.0. When we base the decision of opening a charging station on demand, we actually mean that the flow at the time of making the decision suggests a potential demand of some size. We use demand instead of the flow of EVs because demand in kW is more direct and help us shape the model the way it is now. The outcome of this study provides a number of managerial insights such as optimal expansion of power grid and charging stations under limited budget availability, which can effectively aid decision makers to design a robust network to adopt electric vehicles in a given region. Finally, we showed how the power demand variability and vehicle flow rate impact the adoption of electric vehicles in a given region.

The exposition of this paper is as follows. In Section 2, we present the two-stage stochastic program for the electric vehicle charging station expansion planning problem. We then describe the results deduced from a series of computational experiments performed in Section 3. Lastly, we conclude and present avenues for future research in Section

4. The developed hybrid solution approach to solve our optimization model is outlined and detailed in the [appendix](#) in Section 5.

2. Problem description and model formulation

In this section, we present a two-stage stochastic mixed-integer programming (MIP) formulation to establish a dynamic multi-period plan that maximizes the expected monetary return from expanding power cells and electric vehicle charging stations over a pre-specified planning horizon. We first make electric power capacity expansion decisions to support the installation of charging stations. We represent the power network as a grid where we let $\mathcal{I} = \{2, \dots, |\mathcal{I}| - 1\}$ be the set of candidate rows and $\mathcal{J} = \{2, \dots, |\mathcal{J}| - 1\}$ be the set of candidate columns to consider for possible power expansion of electric vehicle charging stations over a set of time periods $t \in \mathcal{T}$ where $\mathcal{T} = \{1, 2, \dots, T\}$. Each cell $(i, j) \in (\mathcal{I}, \mathcal{J})$ is referred to by its respective row i and column number j . We further define \mathcal{I}_k (indexed by $k \in \mathcal{I}_i$) and \mathcal{J}_l (indexed by $l \in \mathcal{J}_j$) be the neighboring cells of a selected cell $(i, j) \in (\mathcal{I}, \mathcal{J})$ where $(l, k) \neq (i, j)$. We assume that f_{ijt} is the projected expected number of cars that will flow into each cell $(i, j) \in (\mathcal{I}, \mathcal{J})$ in a given time period $t \in \mathcal{T}$. This flow generates a profit of m_{ijt} for the charging stations, if a station is located at cell $(i, j) \in (\mathcal{I}, \mathcal{J})$ in time period $t \in \mathcal{T}$. Locating a charging station at $(i, j) \in (\mathcal{I}, \mathcal{J})$ in time $t \in \mathcal{T}$ requires an expansion of the power network which incurs a fixed investment cost c_{ijt} . We assume we are given a budget B_t^e to select cells for expanding power for electric vehicle charging stations in a given time period $t \in \mathcal{T}$. The model is designed so that if a cell is selected, the set of surrounding cells $(k, l) \in (\mathcal{I}_i, \mathcal{J}_j)$ to the selected cell $(i, j) \in (\mathcal{I}, \mathcal{J})$ are prohibited from being chosen for power expansion

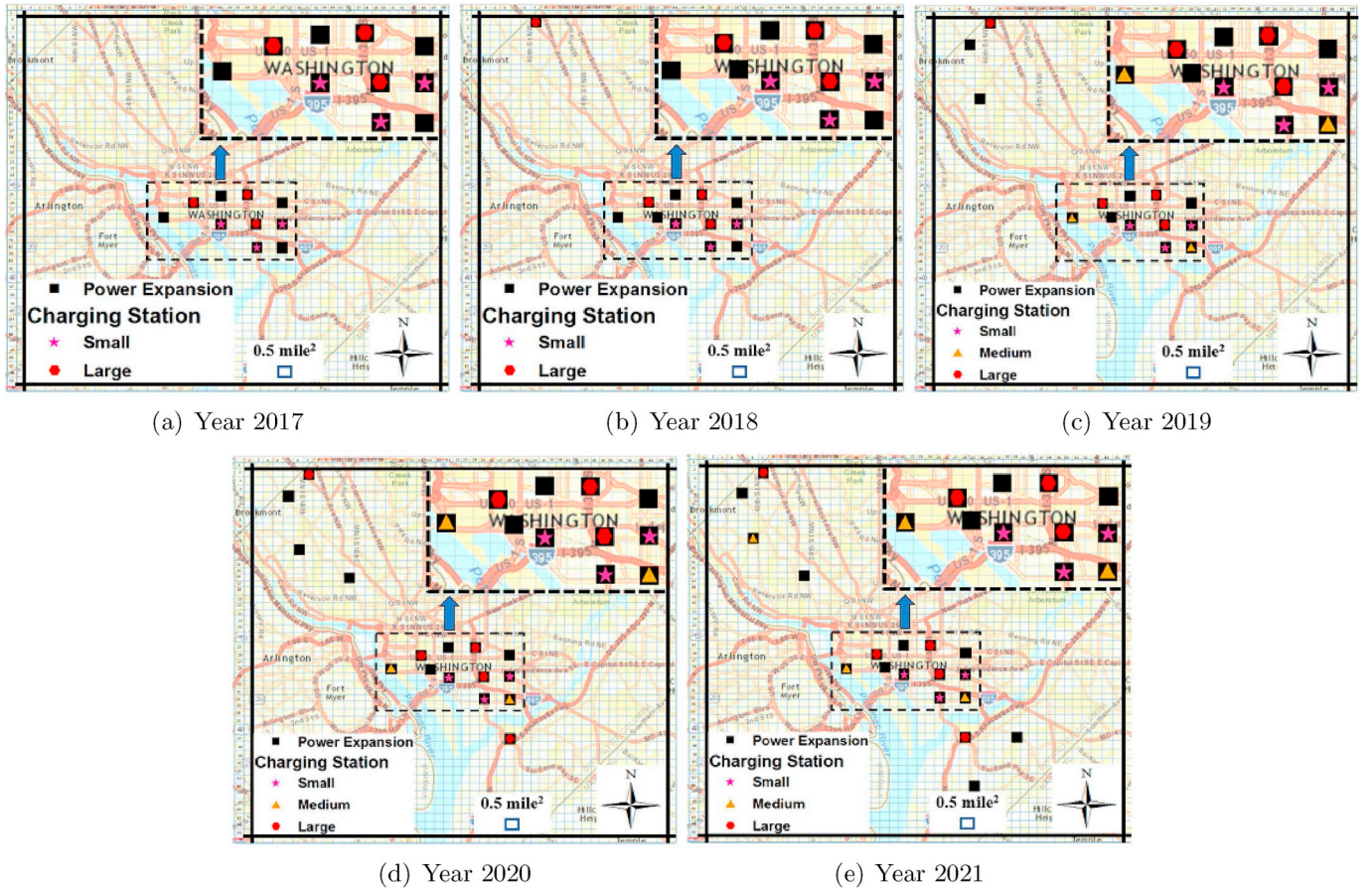


Fig. 5. Electric vehicle charging station expansion planning under scenario 2.

to ensure the sparsity of the charging stations. We feel this is necessary at the early stages of building the infrastructure for electric vehicles, since the adoption rate of electric cars increase steadily. Moreover, sparsity ensures that the covering of demand will not be exaggerated.

After decision makers finish their assessment and projections of electric vehicle flow (f_{ij}), they determine which cells to expand the power capacity. However, there is uncertainty about what the true power demand (in kWh) will be on each cell based on uncertain electric flows. Thus, we denote the realized power demand by d_{ijt}^{ω} . Let Ω be the set of scenarios of different realization of power demand for the charging stations located in cell $(i, j) \in (\mathcal{I}, \mathcal{J})$ at a given time period $t \in \mathcal{T}$ and $\omega \in \Omega$ defines a particular realization. Let ϕ_{st} be the cost of opening a charging station of size $s \in \mathcal{S}$ in time period $t \in \mathcal{T}$, and at that time period, we are given a budget B_t^c to open the charging stations. Since the power demand is stochastic, the amount of power may transfer from cell $(k, l) \in (\mathcal{I}, \mathcal{J})$ to cell $(i, j) \in (\mathcal{I}, \mathcal{J})$ in time period $t \in \mathcal{T}$ under scenario $\omega \in \Omega$ by incurring a reallocation cost of c_{ijkl}^r . This in turn will increase the income (in \$/kWh) of a charging station by serving additional customers visited at cell $(i, j) \in (\mathcal{I}, \mathcal{J})$ in time period $t \in \mathcal{T}$ and is denoted by ψ_{ijkl} . Thus, an expected profit of $(\psi_{ijkl} - c_{ijkl}^r)$ is obtained by reallocating power in the charging stations located at cell $(i, j) \in (\mathcal{I}, \mathcal{J})$ from cell $(k, l) \in (\mathcal{I}, \mathcal{J})$ in time period $t \in \mathcal{T}$. Note that the cells will also have the option to retain their excess energy which they can use in remaining time periods. We make the following additional assumptions to simplify our modeling approach: Electric car traffic volume will increase over time and is certain. This assumption is consistent with the assumption made by Chung and Kwon (2015). Grid power is available throughout the entire time horizon i.e., no disruption will occur during the time horizon that causes power failure. Also, the number of time stages is predetermined and each time stage has an

equal length. All charging stations will be of fast charging DC chargers (referred to as Type 3). This assumption is made to ensure the ability to meet the demand. The power company and charging station investors are assumed to work in coordination and decisions for power expansion are made collaboratively. Finally, charging stations will only be open from the cells whose capacity was expanded in the first-stage.

Let us now introduce the following notation for our two-stage stochastic programming model formulation:

Sets:

- \mathcal{I} : set of rows
- \mathcal{J} : set of columns
- \mathcal{I}_i : set of neighboring rows of row $i \in \mathcal{I}$
- \mathcal{J}_j : set of neighboring columns of column $j \in \mathcal{J}$
- \mathcal{T} : set of time periods
- \mathcal{S} : set of capacities for charging stations
- Ω : set of scenarios

Parameters:

- c_{ijt} : fixed cost of expanding power in cell $(i, j) \in (\mathcal{I}, \mathcal{J})$ in time period $t \in \mathcal{T}$
- m_{ijt} : expected profit from car traffic in dollars for cell $(i, j) \in (\mathcal{I}, \mathcal{J})$ in time period $t \in \mathcal{T}$
- B_t^c : budget availability for expansion in time period $t \in \mathcal{T}$
- f_{ijt} : flow (cars/time period) at cell $(i, j) \in (\mathcal{I}, \mathcal{J})$ in time period $t \in \mathcal{T}$
- ϕ_{st} : cost of opening a charging station of size $s \in \mathcal{S}$ in time period $t \in \mathcal{T}$
- B_t^l : budget availability for locating charging stations in time period $t \in \mathcal{T}$
- c_{ijkl}^r : cost of reallocating power to a charging station located at cell

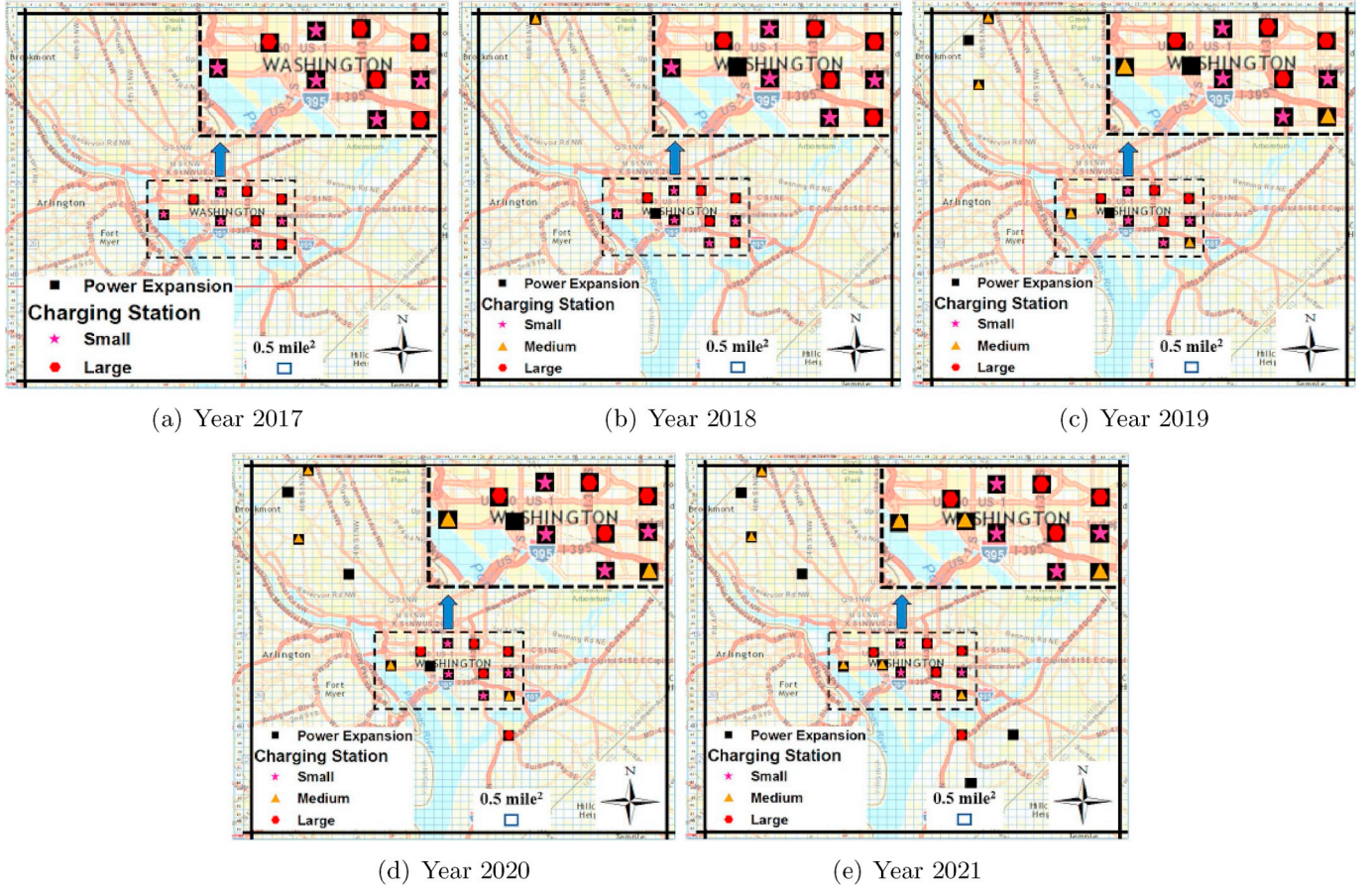


Fig. 6. Electric vehicle charging station expansion planning under scenario 3.

$(i, j) \in (\mathcal{I}, \mathcal{J})$ from cell $(k, l) \in (\mathcal{I}_i, \mathcal{J}_j)$ in time period $t \in \mathcal{T}$

- ψ_{ijklt} : expected income (in \$/kWh) obtained from reallocating power to a charging station located at cell $(i, j) \in (\mathcal{I}, \mathcal{J})$ from cell $(k, l) \in (\mathcal{I}_i, \mathcal{J}_j)$ in time period $t \in \mathcal{T}$
- d_{ijt}^{ω} : power demand (in kWh) at a charging station located in cell $(i, j) \in (\mathcal{I}, \mathcal{J})$ in time period $t \in \mathcal{T}$ under scenario $\omega \in \Omega$
- \bar{c}_{ijs} : capacity (in kWh) of a charging station of size $s \in \mathcal{S}$ located in cell $(i, j) \in (\mathcal{I}, \mathcal{J})$
- γ_{ijt} : minimum utilization required for a charging station located at cell $(i, j) \in (\mathcal{I}, \mathcal{J})$ in time period $t \in \mathcal{T}$
- \bar{p}_{ijt} : amount of residual power available at cell $(i, j) \in (\mathcal{I}, \mathcal{J})$ in time $t = 1$
- α_t : percentage of car charged in time period $t \in \mathcal{T}$
- β : unit power requirement for each car
- ρ_{ω} : probability of scenario $\omega \in \Omega$

Decision Variables:

- X_{ijt} : 1 if cell $(i, j) \in (\mathcal{I}, \mathcal{J})$ is selected for power expansion in time period $t \in \mathcal{T}$; 0 otherwise
- Z_{ijst}^{ω} : 1 if a charging station of size $s \in \mathcal{S}$ is open at cell $(i, j) \in (\mathcal{I}, \mathcal{J})$ in time period $t \in \mathcal{T}$ under scenario $\omega \in \Omega$; 0 otherwise
- Y_{ijklt}^{ω} : amount of power transferred from cell $(k, l) \in (\mathcal{I}_i, \mathcal{J}_j)$ to cell $(i, j) \in (\mathcal{I}, \mathcal{J})$ in time period $t \in \mathcal{T}$ under scenario $\omega \in \Omega$
- P_{ijt}^{ω} : amount of power remaining at cell $(i, j) \in (\mathcal{I}, \mathcal{J})$ in time period $t \in \mathcal{T}$ under scenario $\omega \in \Omega$

We now introduce the following first and second-stage decision variables for our two-stage stochastic programming model formulation. The first-stage decision variables $\mathbf{X} := \{X_{ijt} | (i, j) \in (\mathcal{I}, \mathcal{J}), t \in \mathcal{T}\}$ select the set of cells for possible power expansion of electric vehicle

charging stations in a given time period t . The first set of second-stage decision variables $\mathbf{Z} := \{Z_{ijst}^{\omega} | (i, j) \in (\mathcal{I}, \mathcal{J}), s \in \mathcal{S}, t \in \mathcal{T}, \omega \in \Omega\}$ select the size, cell, and time to open a charging station in a given scenario. The next second-stage decision variables include $\mathbf{Y} := \{Y_{ijklt}^{\omega} | (i, j) \in (\mathcal{I}, \mathcal{J}), (k, l) \in (\mathcal{I}_i, \mathcal{J}_j), t \in \mathcal{T}, \omega \in \Omega\}$ denote the amount of power transferred from cell $(k, l) \in (\mathcal{I}_i, \mathcal{J}_j)$ to cell $(i, j) \in (\mathcal{I}, \mathcal{J})$ in time period $t \in \mathcal{T}$ under scenario $\omega \in \Omega$ and $\mathbf{P} := \{P_{ijt}^{\omega} | (i, j) \in (\mathcal{I}, \mathcal{J}), t \in \mathcal{T}, \omega \in \Omega\}$ denote the amount of power remaining at cell $(i, j) \in (\mathcal{I}, \mathcal{J})$ in time period $t \in \mathcal{T}$ under scenario $\omega \in \Omega$.

The objective function of the electric vehicle power expansion model [EVP] maximizes the first-stage profits and the expected value of the random second-stage profits. The first-stage decisions include the cells to select for power expansion that maximizes the monetary returns from electric vehicle flow at each cell in a given time horizon. These decisions are required to be made prior to a realization of any uncertainty. However, after the uncertainty is revealed the second stage decisions are made which include the charging stations to open from selected first-stage cells, power transferred, and remain in a given cell at a particular time period. The following is a two-stage stochastic mixed-integer linear programming (MILP) model formulation of the problem referred to as model [EVP]:

$$[\text{EVP}] \text{Maximize } \sum_{(i,j) \in (\mathcal{I}, \mathcal{J})} \sum_{t \in \mathcal{T}} m_{ijt} X_{ijt} + \sum_{\omega \in \Omega} \rho_{\omega} Q(\mathbf{X}, \omega) \quad (1)$$

Subject to

$$\sum_{(i,j) \in (\mathcal{I}, \mathcal{J})} c_{ijt} X_{ijt} \leq B_t^e \quad \forall t \in \mathcal{T} \quad (2)$$

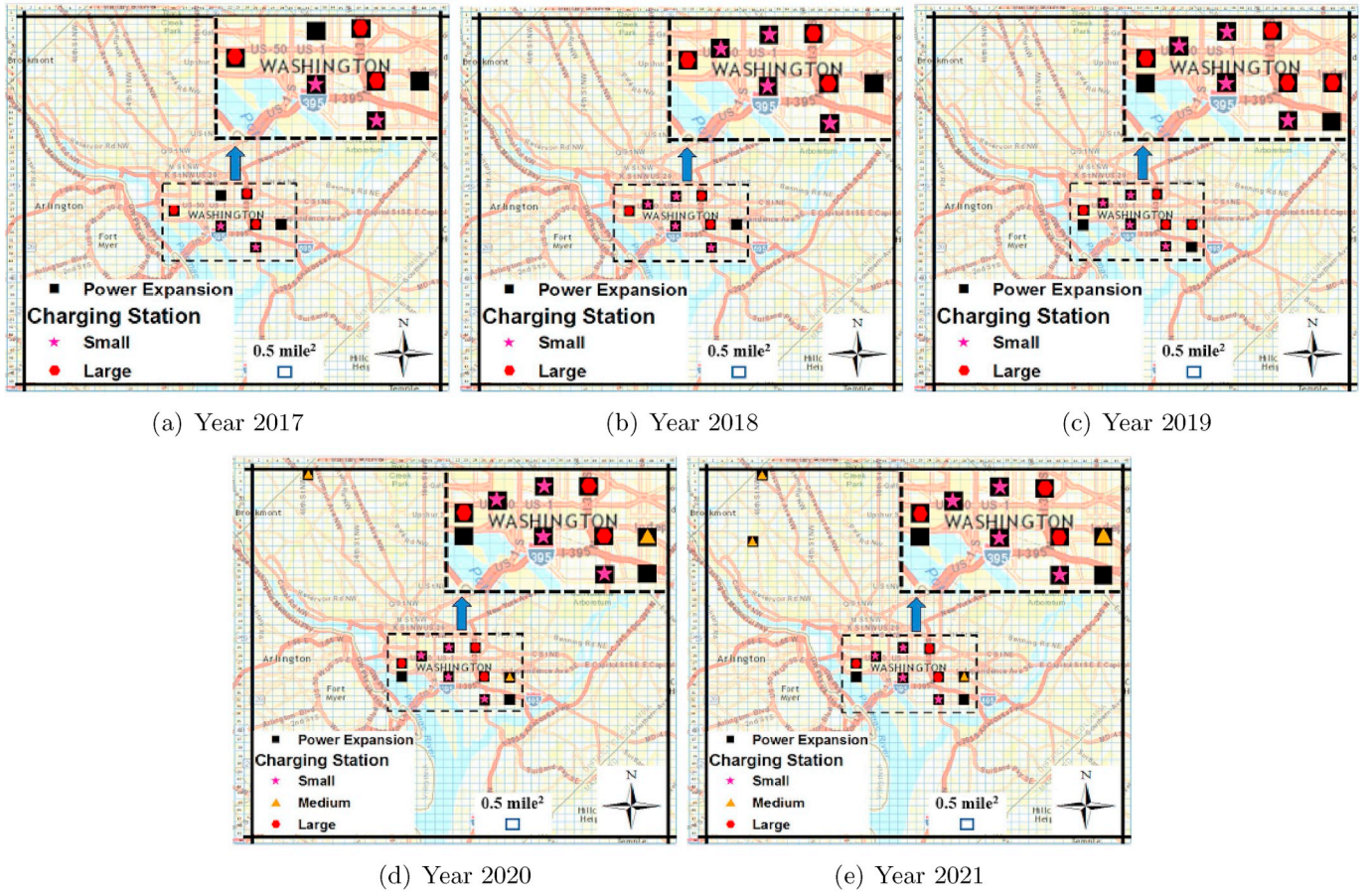


Fig. 7. Impact of low power demand variability on system performance.

$$\sum_{k=i-1}^{i+1} \sum_{l=j-1}^{j+1} X_{klt} \leq 1 \quad \forall (i, j) \in (\mathcal{I}, \mathcal{J}), t \in \mathcal{T} \quad (3)$$

$$X_{ijt-1} \leq X_{ijt} \quad \forall (i, j) \in (\mathcal{I}, \mathcal{J}), t \in \mathcal{T} \quad (4)$$

$$X_{ijt} \in \{0,1\} \quad \forall (i, j) \in (\mathcal{I}, \mathcal{J}), t \in \mathcal{T} \quad (5)$$

with $Q(\mathbf{X}, \omega)$ being the solution of the following second-stage problem:

$$Q(\mathbf{X}, \omega) = \underset{Y, Z, P}{\text{Maximize}} \sum_{(i,j) \in (\mathcal{I}, \mathcal{J})} \sum_{\substack{(k,l) \in (\mathcal{I}, \mathcal{J}) \\ (k,l) \neq (i,j)}} \sum_{t \in \mathcal{T}} (\psi_{ijklt} - c_{ijklt}^r) Y_{ijklt}^\omega \quad (6)$$

$$\text{Subject to} \\ \sum_{(i,j) \in (\mathcal{I}, \mathcal{J})} \sum_{s \in \mathcal{S}} \phi_{st} Z_{ijst}^\omega \leq B_i^c \quad \forall t \in \mathcal{T}, \omega \in \Omega \quad (7)$$

$$\sum_{s \in \mathcal{S}} Z_{ijst}^\omega \leq 1 \quad \forall (i, j) \in (\mathcal{I}, \mathcal{J}), t \in \mathcal{T}, \omega \in \Omega \quad (8)$$

$$Z_{ijst-1}^\omega \leq Z_{ijst}^\omega \quad \forall (i, j) \in (\mathcal{I}, \mathcal{J}), s \in \mathcal{S}, t \in \mathcal{T}, \omega \in \Omega \quad (9)$$

$$\frac{d_{ijt}^\omega X_{ijt}}{\bar{c}_{ijs}} \geq \gamma_{ijt} Z_{ijst}^\omega \quad \forall (i, j) \in (\mathcal{I}, \mathcal{J}), s \in \mathcal{S}, t \in \mathcal{T}, \omega \in \Omega \quad (10)$$

$$\sum_{k=i-1, i \neq k}^{i+1} \sum_{l=j-1, j \neq l}^{j+1} Y_{ijklt}^\omega \leq P_{ijt}^\omega \quad \forall (i, j) \in (\mathcal{I}, \mathcal{J}), t \in \mathcal{T}, \omega \in \Omega \quad (11)$$

$$P_{ijt-1}^\omega - \sum_{k=i-1, i \neq k}^{i+1} \sum_{l=j-1, j \neq l}^{j+1} Y_{ijklt}^\omega = P_{ijt}^\omega \quad \forall (i, j) \in (\mathcal{I}, \mathcal{J}), t \in \mathcal{T}, \omega \in \Omega \quad (12)$$

$$P_{ijt}^\omega = \bar{P}_{ijt} \quad \forall (i, j) \in (\mathcal{I}, \mathcal{J}), t = 1, \omega \in \Omega \quad (13)$$

$$\max\{d_{ijt}^\omega - \beta \alpha_t f_{ijt}, 0\} X_{ijt} \geq \sum_{k=i-1, i \neq k}^{i+1} \sum_{l=j-1, j \neq l}^{j+1} Y_{ijklt}^\omega \quad \forall (i, j) \in (\mathcal{I}, \mathcal{J}), t \in \mathcal{T}, \omega \in \Omega \quad (14)$$

$$Z_{ijst}^\omega \in \{0,1\} \quad \forall (i, j) \in (\mathcal{I}, \mathcal{J}), s \in \mathcal{S}, t \in \mathcal{T}, \omega \in \Omega \quad (15)$$

$$Y_{ijklt}^\omega \geq 0 \quad \forall (i, j) \in (\mathcal{I}, \mathcal{J}), (k, l) \in (\mathcal{I}, \mathcal{J}), t \in \mathcal{T}, \omega \in \Omega \quad (16)$$

$$P_{ijt}^\omega \geq 0 \quad \forall (i, j) \in (\mathcal{I}, \mathcal{J}), t \in \mathcal{T}, \omega \in \Omega \quad (17)$$

The objective function (1) is the sum of the first-stage profits and the expected second-stage profits. The first-stage profits maximize the monetary return that the charging stations may get by expanding power in a given cell $(i, j) \in (\mathcal{I}, \mathcal{J})$ in time period $t \in \mathcal{T}$. Constraints (2) limit the number of cells that can be selected in a given time period $t \in \mathcal{T}$ with a pre-specified budget B_i^c . To ensure that the distribution of charging stations around a selected cell $(i, j) \in (\mathcal{I}, \mathcal{J})$ is sparse, constraints (3) prevent a set of surrounding cells from being chosen for power expansion. The summation limits and the number of stations allowed can be adjusted based on how the sparsity of the selected cell is desired. Constraints (4) indicate that once a cell is expanded for power expansion, it will still be selected in the subsequent time periods. Constraints (5) set the binary restrictions for the first-stage decision variables.

The objective function of the second-stage (6) maximizes the return of rerouting power to cover extra demand. Constraints (7) limit the number of charging stations that can be opened in a given time period $t \in \mathcal{T}$ with a pre-specified budget B_i^c . Constraints (8) ensure that at most one charging station of size $s \in \mathcal{S}$ is opened in a given cell $(i, j) \in (\mathcal{I}, \mathcal{J})$ in time period $t \in \mathcal{T}$ under scenario $\omega \in \Omega$. Constraints (9) indicate that if a

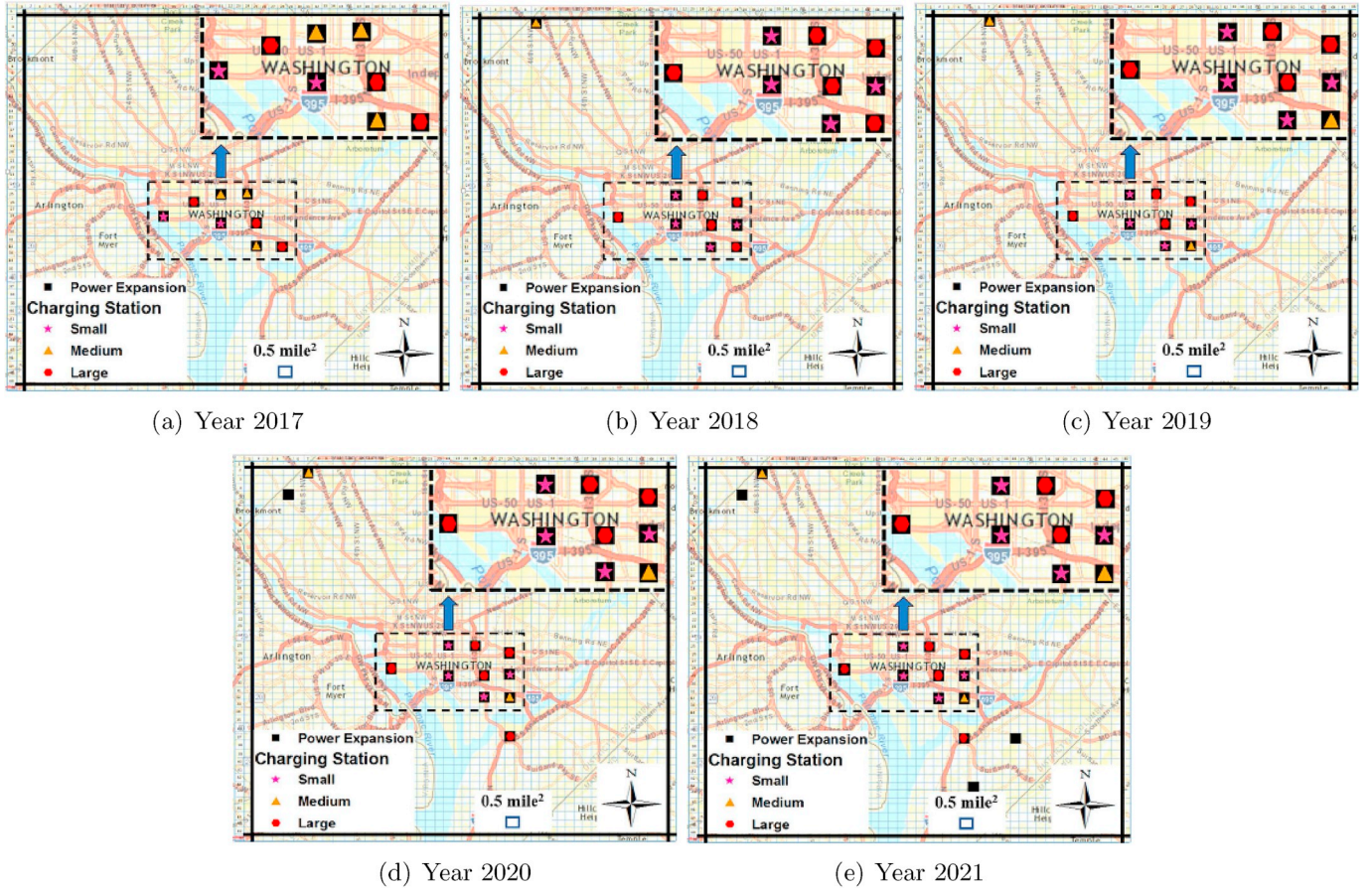


Fig. 8. Impact of high power demand variability on system performance.

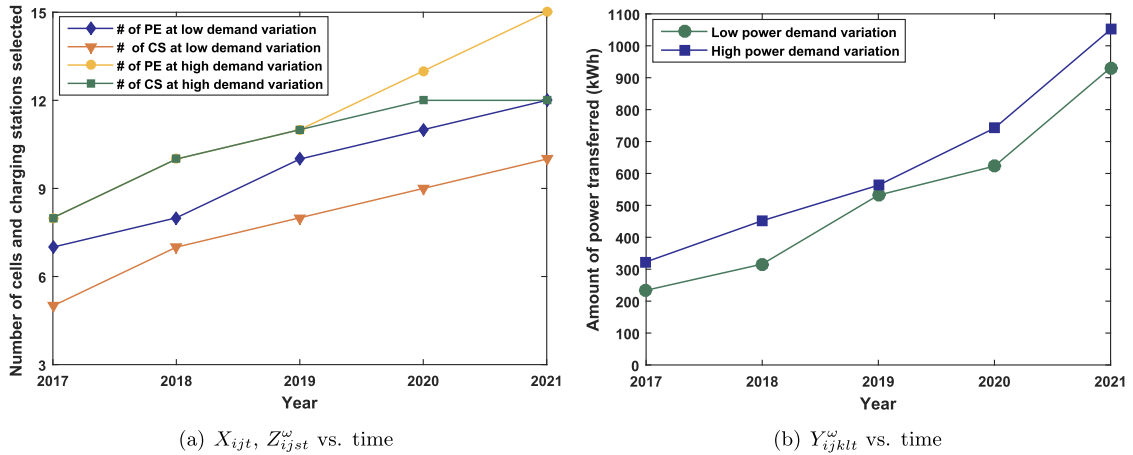


Fig. 9. Impact of power demand variability on system performance.

charging station is opened at time period $t - 1$ then it will still remain open in the subsequent time periods $t \in \mathcal{T}$. Constraints (10) indicate that a charging station is open only if the expected utilization is attractive for the investors. Since power can be drawn from adjacent cells $(k, l) \in (\mathcal{I}_i, \mathcal{J}_j)$ as necessary, the remaining amount should be monitored. Therefore, constraints (11) ensure that the power rerouted is no more than what is available. Constraints (12) assign the remaining power after re-allocation to the next time period. Constraints (13) indicate that the residual power at the first time period is initialized with the parameter \bar{p}_{ij1} , which is the amount of residual power available at the beginning. Constraints (14) ensure that if the demand, which is stochastic in nature, is

more than the expected flow, then power from adjacent cells $(k, l) \in (\mathcal{I}_i, \mathcal{J}_j)$ can be rerouted to the selected cell $(i, j) \in (\mathcal{I}, \mathcal{J})$ to fulfill the unaccounted increase in demand. Note that β and α_t denote the unit power requirement for each car and a percentage of electric car f_{ijt} charged in time period $t \in \mathcal{T}$, respectively. Finally, constraints (15) set the binary restrictions and (16), (17) are the standard non-negativity constraints.

3. Experimental results

This section presents our computational experience in solving model

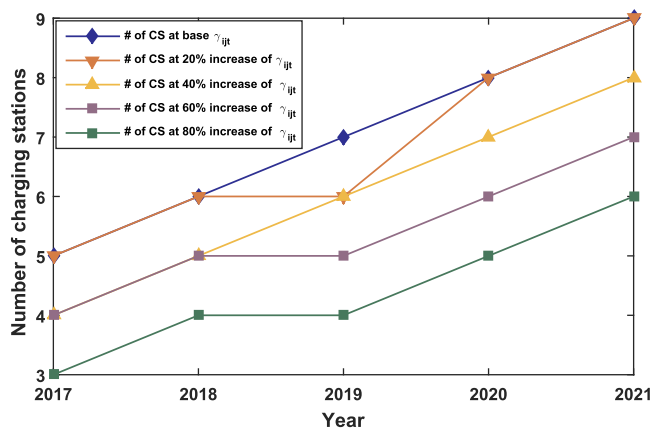


Fig. 10. Impact of γ_{ijt} on locating station decisions.

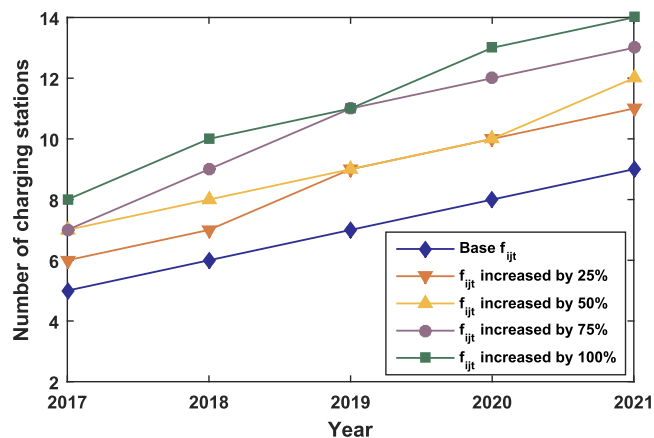


Fig. 11. Impact of f_{ijt} on locating charging station decisions.

[EVP] to test the performance of the algorithms proposed in Section 5 and to draw managerial insights. All the algorithms are coded in GAMS 24.2.1 (General Algebraic Modelin, 2013) and executed on a desktop computer with an Intel Core i7 3.50 GHz processor and 16.0 GB RAM. The optimization solver used is ILOG CPLEX 12.6. The following subsections describe the input parameters used in this study followed by the results obtained from the experimental study and then reports the computational performance of the hybrid Sample Average approximation based Progressive Hedging algorithm to solve model [EVP].

3.1. Input parameters

The region of interest for our case study is Washington, DC for which a network representation is depicted in Fig. 2(a). The demand distribution for Washington, DC is shown in Fig. 2(b). The rationale behind selecting Washington, DC is that the city offers incentives to own electric vehicle cars and the adoption rate is high. The map is divided into a grid of size 50×46 cells (i.e., $|\mathcal{I}| = 50$, $|\mathcal{J}| = 46$) where each cell contributes an area of approximately 0.5 mile^2 . Note that the data for cell-specific parameters are only obtained for those that have a road passing through them; otherwise, the values for the cells are set to zero. We assume that only the active cells can be considered for power expansion and a potential location of opening a charging station. We are considering a 5-year planning horizon starting in 2017 and ending in 2021. All costs are calculated based on 2017 dollars. Costs and profits are then adjusted for inflation. The cost of expanding power (c_{ijkt}) in a given cell $(i, j) \in (\mathcal{I}, \mathcal{J})$ is set to \$700,000 (Institute for Renewable Energy, 2016) and we assume that we are given an annual budget ($B_i^e = \$5M, \$6M, \$7M, \$8M, \text{ and } \$9M$) to expand power for years 2017–2021 (Institute for Renewable Energy, 2016). Similarly, the construction cost for locating a fast electric vehicle charging station (ϕ_{st}) in a new location is set to \$50,000 (Agenbroad and Holland, 2014). We consider three different electric vehicle charging station capacities ($s = 100 \text{ kWh}, 200 \text{ kWh}, \text{ and } 300 \text{ kWh}$). We assume that we are given an annual budget ($B_i^c = \$400, \$550, \$700, \$850, \text{ and } \$1000$) (in thousand dollars) to build infrastructures for electric vehicle charging stations in our tested region for years 2017–2021 (Clean Technica,

² We represent each cell by a virtual region on the map which can be distinct depending on the population, road condition, and power availability in that cell. Our study assumes that each cell contributes an area of approximately 0.5 mile^2 . We further mentioned in our manuscript that the data for cell-specific parameters are obtained for those that have a road passing through them; otherwise, the values for the cells are set to zero. We assume that only the active cells can be considered for power expansion and a potential location of opening a charging station. Finally, it can be noted that the cells can be of any shape as needed though we used squares in our study.

2016). The cost of reallocating power (α_{ijklt}) to a charging station located at cell $(i, j) \in (\mathcal{I}, \mathcal{J})$ from cell $(k, l) \in (\mathcal{I}, \mathcal{J})$ in time period $t \in \mathcal{T}$ is set to \$0.12/kWh (National Public Radio, 2016). Finally, we set $m_{ijt} = \$0.5/\text{kWh}$, $\gamma_{ijt} = 40\%$, $\beta = 10 \text{ kWh}$, and $\alpha_t = 20\%$ for our base case experimentations.

3.2. Experimental results

3.2.1. Impact of B_i^e and B_i^c on system performance

To understand the impact of the power expansion (B_i^e) and charging station (B_i^c) budgets on system performance, we conduct four different experiments: (a) base budget for power expansion and charging station, (b) B_i^c is increased by 50% while keeping the budget B_i^e fixed, (c) B_i^e is increased by 50% while keeping the budget B_i^c fixed, and (d) both B_i^e and B_i^c are increased by 50%. Table 1 summarizes the test instances of different budgets for power expansion and charging stations from 2017 to 2021. Figs. 3–6 show the deployment of power expansion cells X_{ijt} (represented by symbol “□” in Figs. 3–6) and charging stations Z_{ijst}^ω (represented by symbol “○” in Figs. 3–6) for these experiments. Clearly, the decisions of X_{ijt} and Z_{ijst}^ω are highly impacted by the budgets B_i^e and B_i^c set by the decision makers. It is observed that the results for scenario 1 (shown in Fig. 4) show a little progression of selecting charging stations over the base case scenario (shown in Fig. 3). This is because scenario 1 kept the budget for power expansion B_i^e fixed; thus, the model gets less options to establish charging stations in the second-stage even though there may still be money in the budget B_i^c to open charging stations. We now see that a wide-spread distribution of cells for power expansion are getting selected under scenario 2 (shown in Fig. 5). However, it is important to note that many of the cells selected in the first-stage are eventually not picked for locating charging stations in the second-stage. This is because of the lack of money available in the budget to open charging stations under this scenario. Finally, we observe a rapid expansion of power cells and charging stations for the case when we assume that both the budgets, B_i^e and B_i^c , are allowed to be increased by 50% over years 2017–2021 (scenario 3), and the results are illustrated in Fig. 6. We observe some additional charging stations being located far away from the original cluster of stations primarily due to serving the high density of population, hospitals, and colleges located near the stations. In summary, it is observed that depending on the values of B_i^e and B_i^c set by the decision maker many more cells and charging stations are opened to provide a broader coverage for the electric vehicles. These results shall further provide an insightful ground for decision makers to invest in power expansion that supports the adoption of electric vehicles in the long run.

3.2.2. Impact of power demand (d_{ijt}^ω) variability on system performance

The second set of experiments shows how different power demand

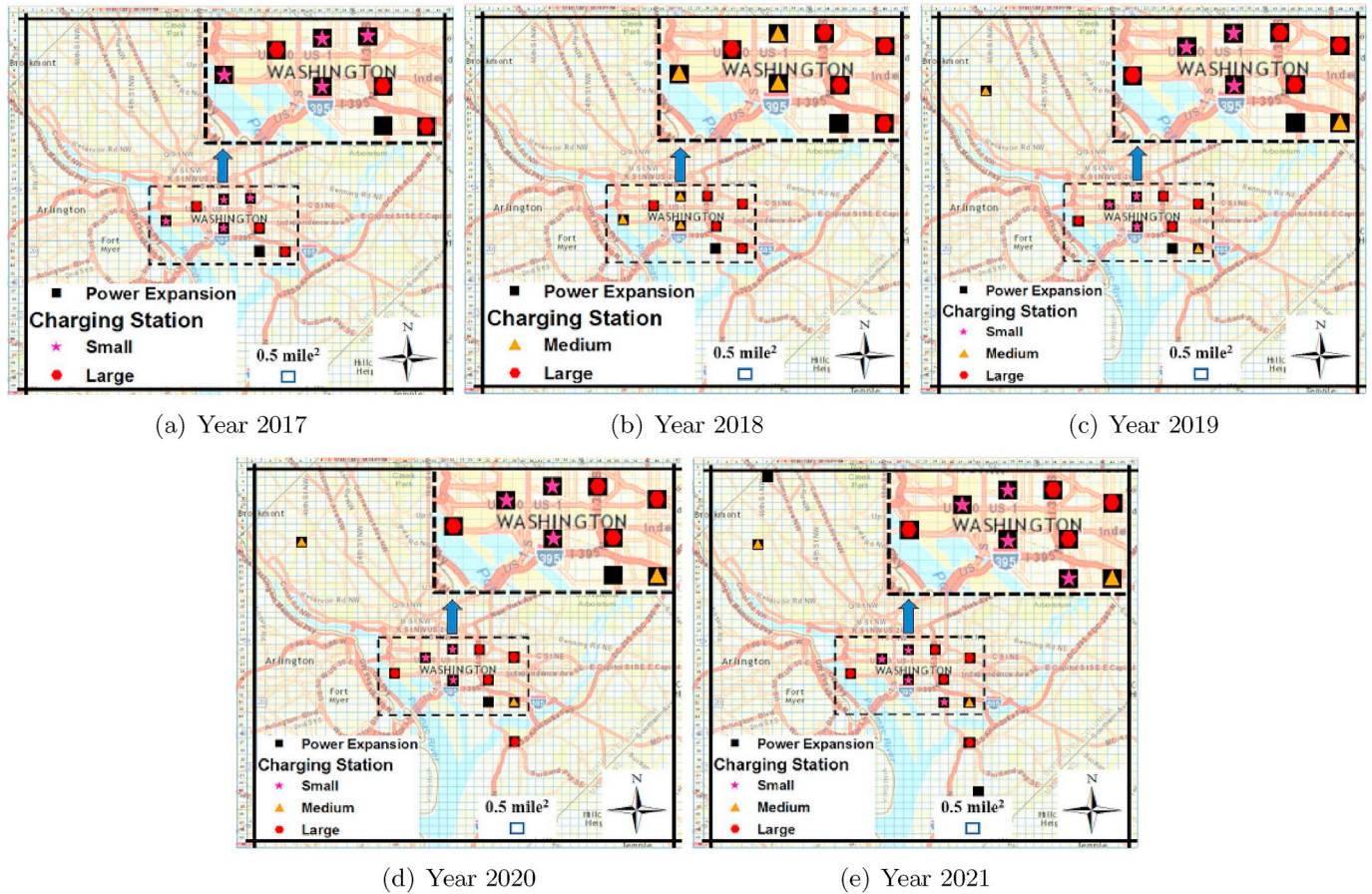


Fig. 12. Impact of 50% increase in f_{jt} on system performance.

Table 2
Problem size of the test instances.

Case	$ \mathcal{I} $	$ \mathcal{J} $	$ \mathcal{S} $	Binary Variables	Continuous Variables	Total Variables	No. of Constraints	
1	26	24	3	5	12,480	1,950,000	1,962,480	56,170
2	26	24	3	10	24,960	3,900,000	3,924,960	112,340
3	38	35	3	5	26,600	8,851,150	8,877,750	99,760
4	38	35	3	10	53,200	17,702,300	17,755,500	199,520
5	50	46	3	5	46,000	26,461,500	26,507,500	172,510
6	50	46	3	10	92,000	52,923,000	53,015,000	345,020

(d_{ijt}^{ω}) variation levels impact electric vehicle expansion decisions. Electricity demand for charging stations cannot be accurately predicted in advance. Therefore, the electricity demand is modeled as a random variable of which probability distribution may not be known in advance. Thus, a set of scenarios Ω of different realization of power demand for the EV charging stations is defined, where each scenario $\omega \in \Omega$ is associated with a positive probability p_{ω} ($\sum_{\omega \in \Omega} p_{\omega} = 1$). Therefore, a large set of scenarios are required to accurately estimate stochastic demand. To handle this complexity, Monte Carlo simulation is implemented for generating scenarios of demand. The generated samples are independent and identically distributed (iid) random variables. Moreover, we assume EV power demand follows a multi-variate normal distribution $N(\mu, \Xi)$ in each time period, where vectors μ and Ξ are defined as the forecasted EV power demand and forecasting error, respectively. It is worth noting that the error terms are also considered to be independent and normally distributed with mean zero and variance σ^2 . the demand for each period is independent and varies in the range $[\bar{d}_{ijt}(1 - \epsilon), \bar{d}_{ijt}(1 + \epsilon)]$ for each cell $(i, j) \in (\mathcal{I}, \mathcal{J})$ in time period $t \in \mathcal{T}$. Note that \bar{d}_{ijt} represents the nominal power demand for

each cell $(i, j) \in (\mathcal{I}, \mathcal{J})$ in time period $t \in \mathcal{T}$ and we assume that the demands are uniformly distributed. We create two different realistic scenarios where we set $\epsilon = 50\%$ and $\epsilon = 15\%$ to represent *high* and *low* power variation levels, respectively. Note that there are a number of factors that may govern the power variability in a given region, such as the availability of electric cars and among them the percentage that charge at the charging stations located in the service region. Moreover, customers' willingness to buy, along with the availability of federal tax credits, state and/or local incentives, and auto manufacturer incentives for electric and plug-in hybrid vehicles, all play a major role in the availability of electric cars in a given region. Figs. 7 and 8 demonstrate the network under low and high power demand variation levels. Results indicate that the number of cells for power expansion and charging station increases with the increase in variability of power demand under a specified budget limit. More specifically, the model decides to expand 18.75% power cells and 35.89% charging stations to counter high power demand variability over the base case scenario. Fig. 9(a) summarizes the number of power expansion cells (PE) and charging stations (CS) opened under low and high demand variabilities. This in turn will have an impact on the amount of power transferred from cell $(i, j) \in (\mathcal{I}, \mathcal{J})$ to cell $(k, l) \in (\mathcal{I}, \mathcal{J})$ under scenario $\omega \in \Omega$, as illustrated in Fig. 9(b). Overall, we observe that the power demand variability levels highly impact the electric vehicle expansion plans.

3.2.3. Impact of γ_{ijt} on system performance

To see the impact of minimum utilization of the charging station γ_{ijt} on system performance, we conduct a series of experiments by increasing the value of γ_{ijt} from 20% to 80%. Fig. 10 demonstrates a relationship between charging station opening decisions Z_{ijst}^{ω} under different γ_{ijt} values. It is clear from the figure that when the value of γ_{ijt} increases, the charging station opening decisions Z_{ijst}^{ω} decreases. For

Table 3
Performance of enhancement techniques used in [PHA].

Case	N	[PHA]			[PHA + HR]			[PHA + HR + RHA]		
		GAP (%)	CPU (sec)	Iter	GAP (%)	CPU (sec)	Iter	GAP (%)	CPU (sec)	Iter
1	20	9.07	10,800	37	0.97	789	12	0.83	642	4
	30	11.47	10,800	41	0.96	932	8	0.91	847	3
	40	12.32	10,800	27	0.98	1063	9	0.87	984	5
2	20	8.43	10,800	32	0.86	1532	11	0.81	1238	4
	30	11.65	10,800	35	0.92	1784	13	0.85	1453	3
	40	17.82	10,800	43	0.96	2145	11	0.79	1703	2
3	20	7.28	10,800	25	0.69	1368	7	0.84	1029	3
	30	9.69	10,800	19	0.93	1598	9	0.82	1386	4
	40	15.34	10,800	26	0.87	1782	6	0.77	1839	3
4	20	10.07	10,800	37	0.94	4758	13	0.84	2742	3
	30	12.35	10,800	43	0.83	6436	9	0.94	4332	2
	40	9.67	10,800	32	0.97	8643	11	0.79	6863	4
5	20	10.07	10,800	23	0.96	6989	7	0.9	5328	3
	30	12.35	10,800	25	0.83	8236	9	0.84	5384	4
	40	9.67	10,800	19	3.65	10,800	6	0.88	6547	5
6	20	23.67	10,800	24	5.99	10,800	8	0.94	8724	7
	30	18.35	10,800	19	10.35	10,800	7	0.87	9524	4
	40	15.63	10,800	27	14.94	10,800	21	1.19	10,800	4
Average		12.49	10,800.0	29.7	2.64	5069.7	9.8	0.87	3964.7	3.7

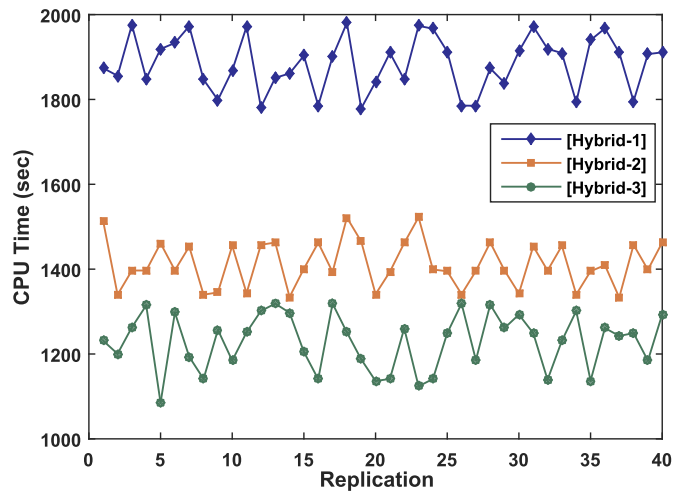


Fig. 13. Comparison of solution time in each replication of the SAA algorithm.

Table 4
Comparison of different solution approaches.

Case	N	M	[SAA]			[Hybrid-1]			[Hybrid-2]			[Hybrid-3]		
			GAP (%)	CPU (sec)	Iter	GAP (%)	CPU (sec)	Iter	GAP (%)	CPU (sec)	Iter	GAP (%)	CPU (sec)	Iter
5	20	5	0.89	9368	1	0.98	8452	2	0.75	6152	1	0.89	4235	1
		10	0.69	10,234	1	0.89	9821	2	0.71	6478	2	0.92	5343	2
	30	5	8.96	10,800	1	7.62	10,800	1	0.83	6992	1	0.94	5862	1
		10	mem ^a	-	-	mem	-	-	2.56	10,800	1	0.88	6686	1
		5	mem	-	-	mem	-	-	0.76	6926	2	0.94	7535	2
6	20	10	mem	-	-	mem	-	-	3.54	10,800	1	0.89	8954	1
		5	7.76	10,800	1	0.66	8452	1	0.65	6124	1	0.79	6628	1
	30	10	mem	-	-	0.69	8821	2	0.81	7720	2	0.86	6992	1
		5	mem	-	-	7.62	10,800	2	0.83	9524	1	0.92	7323	2
		10	mem	-	-	mem	-	-	3.23	10,800	1	0.88	8657	1
40	5	mem	-	-	mem	-	-	4.76	10,800	2	0.94	9875	2	
	10	mem	-	-	mem	-	-	5.67	10,800	1	1.39	10,800	1	
Average			4.58 ^b	10,300.5	1.0	3.08 ^b	9524.3	1.7	2.09	8659.7	1.3	0.94	7407.5	1.3

^a Out of Memory.

^b Instances where (a) did not contribute to the average calculation.

instance, an 80% increase in γ_{ijt} value decreases the average number of charging stations $|Z|$ opening decisions by 37.14%. This indicates the potential of improving the minimum utilization level γ_{ijt} on the system performance.

3.2.4. Impact of f_{ijt} on system performance

We now analyze the impact of vehicle flow, f_{ijt} , on system performance. Estimating f_{ijt} can be challenging and depending on the geometry of the roads (e.g., curvy links) the task can be even more difficult. However, a rough estimation of f_{ijt} can be made as follows: (i) developing a routing algorithm that deploys electric vehicles from multiple source to destination points to get an estimation of the number of vehicles passed through each link of the real world physical network (Chung and Kwon, 2015), and then (ii) developing cells on the network obtained from (i) to estimate the number of electric vehicles passing through each cell in a given time period. Fig. 11 provides a relationship between charging station opening decisions Z_{ijst}^ω under different f_{ijt} values. Clearly, increasing the flow (f_{ijt}) at each cell $(i, j) \in (\mathcal{I}, \mathcal{J})$ in time period $t \in \mathcal{T}$ impacts the charging station opening decisions Z_{ijst}^ω under a pre-specified budget restriction. For instance, a 50% increase in f_{ijt}

increases the average number of charging stations $|Z|$ by 31.4%. A network representation for this scenario is depicted in Fig. 12. It is interesting to note that we observe a widespread distribution of charging stations under this scenario (shown in Fig. 12) compared to the base case scenario (shown in Fig. 3).

3.3. Analyzing the performance of solution algorithms

This section presents our computational experience in solving model [EVP] using the algorithms proposed in Section 5. To help the readers follow our approaches, we have used the following notations to represent the algorithms:

- [SAA]: Sample Average Approximation (SAA) algorithm (described in Section 5.2)
- [PHA]: Progressive Hedging Algorithm (PHA) (described in Section 5.3)
- [Hybrid-1]: Sample average approximation algorithm where the subproblems of the [SAA] are solved using the Progressive Hedging algorithm (PHA) (described in Section 5.3)
- [Hybrid-2]: Sample average approximation algorithm where the subproblems of the [SAA] are solved using an enhanced Progressive Hedging algorithm (PHA) (enhancement techniques described in Sections 5.4.1 and 5.4.2)
- [Hybrid-3]: Sample average approximation algorithm where the subproblems of the [SAA] are solved using an enhanced Progressive Hedging algorithm (PHA) (enhancement techniques described in Sections 5.4.1, 5.4.2, and 5.4.3) The algorithms presented above are terminated when at least one of the following criteria is met: (a) the optimality gap (i.e., $\varepsilon = |UB - LB|/UB$) falls below a threshold value of $\varepsilon = 0.01$; or (b) the maximum time limit $time^{max} = 10,800$ (in CPU seconds); or (c) the maximum number of iterations $iter^{max} = 100$ is reached. To terminate the Progressive Hedging algorithm, we have used additional stopping criteria which are described at the end of Section 5.3. The size of the deterministic equivalent problem of model [CSC] are presented in Table 2.

The first set of experiments (shown in Table 3) examines the impact of different enhancement techniques over the basic Progressive Hedging algorithm ([PHA]). We employ the following enhancement techniques: (i) [PHA + HR] that incorporates penalty parameter updating techniques (described in Section 5.4.1) and heuristics strategies (described in Section 5.4.2) inside the [PHA] algorithm and (ii) [PHA + HR + RHA] that incorporates a rolling horizon algorithm (described in section 5.4.3) along with penalty parameter updating techniques (described in Section 5.4.1) and heuristics strategies (described in Section 5.4.2) inside the [PHA] algorithm. Table 3 presents the computational results obtained from solving model [EVP] using different variants of the [PHA] algorithm (e.g., [PHA + HR], [PHA + HR + RHA]). We consider three different scenario sizes $N = \{20, 30, 40\}$ and tested them in problem cases 1–6 (shown in Table 2) to obtain 18 different problem instances. We do not present the results obtained from CPLEX since CPLEX runs *out of memory* when solving all the problem instances as reported in Table 3. Note that in reporting the computational performance of the algorithms, we highlighted the algorithm which is solved in less than the stopping criteria ε while simultaneously producing the smallest running time (represented by CPU in Table 3) for a given test instance. Otherwise, if such a quality solution is not found within the maximum time or iteration limit then the algorithm with the smallest optimality gap (represented by GAP in Table 3) is highlighted. Results indicate that implementing the enhancement techniques discussed in section 5.4 substantially improves the performance of the Progressive hedging algorithm ([PHA]). More specifically, algorithm [PHA] fails to solve any of the problem instances in less than a 1% optimality gap within the pre-specified time limit, whereas algorithms [PHA + HR] and [PHA + HR + RHA] solve 14 and 17 out of 18 problem instances, respectively by obeying the termination criteria described earlier. On average,

algorithm [PHA + HR + RHA] provides a 21.8% faster solution than algorithm [PHA + HR] and drops the average optimality gap from 2.64% to 0.87%. Note that algorithm [PHA + HR + RHA] does not guarantee to produce a valid lower bound for algorithm [PHA]. Therefore, the results shown in Table 3 use the lower bound of the [PHA + HR] algorithm to present an optimality gap for the [PHA + HR + RHA] algorithm i.e., $100 \cdot (UB_{[PHA+HR+RHA]} - LB_{[PHA+HR]}) / UB_{[PHA+HR+RHA]} \%$. We further point out to the reader that even though algorithm [PHA + HR + RHA] terminates with an ε -optimal solution, the quality of the solution produced by the [PHA + HR + RHA] algorithm, as shown in Table 3, is consistently high.

The second set of experiments analyze the benefits of using different accelerated techniques in each replication of the Sample Average Approximation [SAA] algorithm. Fig. 13 shows the average computing time spent in solving each replication of the [SAA] algorithm using algorithms [Hybrid-1], [Hybrid-2], and [Hybrid-3]. To demonstrate the impact of the accelerated techniques, we pick a small problem instance consisting of $|A| = 14$, $|S| = 13$, $|S^1| = 3$, $|S^2| = 5$, $N = 10$, and $M = 40$. Results indicate that the computation time can be significantly reduced by using algorithm [Hybrid-2] over algorithm [Hybrid-1]. We further observe even more reduction in computing time by employing the rolling horizon framework ([Hybrid-3]) inside algorithm [Hybrid-2]. On average, algorithm [Hybrid-3] is 1.2 and 1.5 times faster than the [Hybrid-2] and [Hybrid-1] algorithms, respectively.

The final set of experiments present the results from solving model [EVP] using the algorithms proposed in Section 5 (shown in Table 4). To test the performance of the algorithms, we use Cases 5 and 6 (the two largest test cases from Table 2) and vary sample size N and replication number M in the [SAA] algorithm to obtain 12 different problem instances. We set the large scenario size $N' = 500$ to evaluate the [SAA] gap. We do not present results obtained from CPLEX since CPLEX runs *out of memory* when solving all the problem instances reported in Table 4. Results indicate that [SAA] is capable of solving only 2 out of 12 problem instances by obeying the pre-specified termination criteria. The performance can be slightly improved by solving the subproblems of the [SAA] algorithm using the [PHA] algorithm. It is observed that algorithm [Hybrid-1] is now able to solve 4 out of 12 problem instances by obeying the pre-specified termination criteria. The benefits of using the algorithms become more evident when the enhancement techniques (described in section 5.4) are implemented in [PHA] algorithm to solve the subproblems of the [SAA] algorithm. The overall average optimality gap for the [Hybrid-2] algorithm is reported as 2.09%, with 7 out of 12 problem instances solved within the pre-specified termination criteria. On the other hand, the overall average optimality gap for the [Hybrid-3] algorithm is reported as 0.94%, with 11 out of 12 problem instances solved in less than a 1.0% optimality gap within the specified time limit. It is important to note that algorithm [Hybrid-3] on average saves 11.7% computation time over algorithm [Hybrid-2] in reporting the optimality gaps presented in Table 4. In summary, algorithm [Hybrid 3] seems to offer high quality solutions consistently within the experimental range.

4. Conclusion

This study develops a novel optimization framework that can be used to design widespread adoption of electric vehicle charging stations for a pre-specified planning horizon subjected to stochastic power demands. A multi-time period two-stage stochastic mixed integer linear programming model is constructed to determine a set of power cells to expand over time so that they can be utilized as potential locations for opening charging stations while simultaneously supporting the stochastic power needs of the stations under uncertainty. The model can be computationally very challenging depending on the size of the cells, time periods, and scenarios set by the decision maker. To alleviate these challenges and to solve real scale problem instances, we develop a

hybrid decomposition algorithm that combines Sample Average Approximation (SAA) with an enhanced Progressive Hedging algorithm (PHA). The hybrid algorithm incorporates several algorithmic improvements such as penalty parameter updating schemes, local and global heuristics, and the rolling horizon heuristic. Computational results showed that the enhanced variant of the hybrid algorithm [Hybrid 3], which incorporates all the enhancement techniques discussed in Section 3.3, can be used to solve realistic instances of large size problems.

By using Washington, DC as a testing ground, we conducted thorough computational experiments to test our model and to draw managerial insights. Our computational experiments reveal some insightful results about the impact of cell expansion (B_i^e) and charging station budgets (B_i^c) on electric vehicle adoption performance. We further conduct sensitivity analysis on the impact of power demand (d_{ijt}^w) variability and vehicle flow rate (f_{ijt}) on system performance. It is observed that the model decides to open an additional 18.75% power expansion cells and 35.89% charging stations to counter high power demand variability over the base case scenario. Moreover, we observe that a 50% increase in vehicle flow f_{ijt} will open an additional 31.4% charging stations in our tested region under a specified budget constraint. We believe our results will help decision makers develop a future sustainable transportation system that will add value not only to the economy but also to the environment.

This research opens up a number of future research opportunities. Our study makes several assumptions that can be made more realistic in future works. For example, the flow of car fluctuates throughout the day and from a month to another. A more realistic approach would be to track the changes in flow at a finer time frame than yearly. This will help in making more robust decisions. Another assumption made is the availability of electric power. Disruptions (from natural disasters, for example) and their effect on the ability to satisfy demand can be studied further. Options that helps in mitigating the absence of electricity can be included to alleviate the situation and satisfy demand as much as possible. Congestion and its effect on the drivers decision to charge the car is another factor of consideration. A game-theoretic approach, where we assume that the decision making entities do not work in

collaboration, would lead to interesting insights into what type of actions would best incentivize the coordination between the two players in order to achieve the idealized scenario. It is also worth to study the multiple customers the power company needs to consider when making a multi-objective decision on where to expand the power grid instead of catering to the charging station needs separately. Since self-driving cars have become a reality, this model can be extended to include autonomous vehicles. Some experts expect that ride sharing will soon become the more popular choice of commute due to the self-driving capability (ArcashingtonA, 2016). This will help in solving issues such as range anxiety and long charging times. Automating transportation will help in making better decisions about the power requirements by linking cars information to the smart grid and scheduling charging sessions ahead of time. This will make EVs more popular and remove the ambiguity of demand to a large extent. Future studies will investigate how the proposed optimization model can be extended to solve the integrated shared problem between autonomous and electrified vehicles. Demand in our work is a prediction of how much electric energy is requested based on the flow of cars, regardless of any abnormal road conditions. Relocation of demand can be considered based on the traffic on road to reflect the different adaptations the drivers make when they encounter difficulties reaching the nearest charging station. The assumption that drivers charge at the nearest charging station can be relaxed to allow preferences of customers and their willingness to deviate from their current behavior in order to visit charging stations. We ignored the interactions taking place between locations when we expand power at a cell. Future works should consider the network interactions of expanding the power grid for delivery of increased flow at multiple locations. High fidelity models will be developed in the future to relax these assumptions. Further, it is interesting to integrate renewable energy sources into the optimization framework and assess the robustness of the model in a situation where a disruption (e.g., hurricane, tornado) impacts the system. Finally, The problem can be modeled as a multi-stage stochastic program to represent the case when the decision maker can adjust decisions based on the output of the previous period or stage. These issues will be addressed in future studies.

Appendix

5.1 Solution approach

By setting $|\Omega| = 1$ and $|\mathcal{T}| = 1$ i.e., a single scenario and a single time period, we can show that the problem [EVP] is a special case of a capacitated facility location problem which is known to be an \mathcal{NP} -hard problem (Magnanti and Wong, 1981). Therefore, commercial solvers, such as CPLEX, can hardly solve a small to moderate sized instance of such problems. This motivates us to develop a hybrid decomposition algorithm that combines a Sample Average Approximation technique with an enhanced Progressive Hedging algorithm. The techniques used to enhance the Progressive Hedging algorithm are local and global adjustment techniques and a rolling horizon algorithm. The goal is to generate high quality solutions for problem [EVP] in a reasonable amount of time.

5.2. Sample average approximation

We first employ a sampling technique, known as the *Sample Average Approximation* (SAA) scheme, to solve problem [EVP]. The idea of the SAA scheme is to generate a random sample and approximate the expected value function by the corresponding sample average function. The procedure is repeated until a pre-specified tolerance gap is achieved. The SAA provides high quality feasible solutions along with the statistical estimation of their optimality gap. The SAA scheme has previously been applied to solve large scale supply chain network flow related problems (see e.g., (Verweij et al., 2003), (Santoso et al., 2005), (Chang et al., 2007), (Schutz et al., 2009)) and the convergence properties and statistical performance of the SAA scheme can be found in Kleywegt et al. (2001), Norkin et al. (1998b) and (Norkin et al., 1998a), and Mark et al. (Mak et al., 1999). The first step of SAA generates random samples with $N < |\Omega|$ realizations of uncertain parameters and then approximates the recourse function with the sample average function $\frac{1}{N} \sum_{n=1}^N Q(\mathbf{X}, n)$. Problem [EVP] is now approximated by the following SAA problem:

$$\text{Maximize}_{\mathbf{X} \in \mathcal{X}} \left\{ \hat{\mathbf{g}}(\mathbf{X}) := \sum_{(i,j) \in (\mathcal{I}, \mathcal{J})} \sum_{l \in \mathcal{T}} m_{ijt} X_{ijt} + \frac{1}{N} \sum_{n=1}^N Q(\mathbf{X}, n) \right\} \quad (18)$$

As the sample size increases the optimal solution of (18), $\hat{\mathbf{X}}_N$, and the optimal value v_N , converges with probability one to an optimal solution of the original problem [EVP] (Kleywegt et al., 2001). Assuming that the SAA problem is solved within an absolute optimality gap $\delta \geq 0$, we can estimate the sample size N needed to guarantee an ε -optimal solution to the true problem with probability at least equal to $(1 - \alpha)$ as:

$$N \geq \frac{3\sigma_{max}^2}{(\varepsilon - \delta)^2} (|\mathcal{I}| |\mathcal{J}| |\mathcal{T}| (\log 2) - \log \alpha) \quad (19)$$

where $\varepsilon > \delta$, $\alpha \in (0,1)$ and σ_{max}^2 is a maximal variance of certain function differences (Kleywegt et al., 2001). Sample size estimation using equation (19) is too conservative for practical applications. Thus, one can choose a sample size N as a trade-off between the solution quality obtained by solving (18) and the computational burden needed to solve it. In each iteration of the algorithmic step, SAA provides a valid statistical lower and upper bound for the original problem [EVP] and the process terminates when the gap between the estimators falls below a pre-specified threshold value.

The following steps briefly summarize the Sample Average Approximation (SAA) technique to solve problem [EVP].

1. Generate M independent demand scenarios of size N i.e., $\{\mathbf{d}_m^1(\omega), \mathbf{d}_m^2(\omega), \dots, \mathbf{d}_m^N(\omega)\}$, $\forall m = 1, \dots, M$, where $\mathbf{d} = \{d_{ijt}^\omega, \forall (i,j) \in (\mathcal{I}, \mathcal{J}), t \in \mathcal{T}, \omega \in \Omega\}$ and solve the corresponding SAA:

$$\underset{\mathbf{X} \in \mathbf{X}}{\text{Maximize}} \left\{ \hat{\mathbf{g}}(\mathbf{X}): = \sum_{(i,j) \in (\mathcal{I}, \mathcal{J})} \sum_{t \in \mathcal{T}} m_{ijt} X_{ijt} + \frac{1}{N} \sum_{n=1}^N Q(\mathbf{X}, n) \right\} \quad (20)$$

The optimal objective value is denoted by \mathbf{v}_N^m and the optimal solution by $\hat{\mathbf{X}}_N^m$; $m = 1, \dots, M$.

2. Compute the average of the optimal solutions obtained by solving all SAA problems, $\bar{\mathbf{v}}_M^N$ and variance, $\sigma_{\bar{\mathbf{v}}_M^N}^2$:

$$\bar{\mathbf{v}}_M^N = \frac{1}{M} \sum_{m=1}^M \mathbf{v}_N^m \quad (21)$$

where, $\bar{\mathbf{v}}_M^N$ provides a statistical upper bound on the optimal objective function value (\mathbf{v}^*) for the original problem defined by (1)–(17) i.e., $\bar{\mathbf{v}}_M^N \geq \mathbf{v}^*$ (Norkin et al., 1998b). Since M samples are generated and $\mathbf{v}_N^1, \mathbf{v}_N^2, \dots, \mathbf{v}_N^M$ are independent, the variance of $\bar{\mathbf{v}}_M^N$ is given by:

$$\sigma_{\bar{\mathbf{v}}_M^N}^2 = \frac{1}{(M-1)M} \sum_{m=1}^M (\mathbf{v}_N^m - \bar{\mathbf{v}}_M^N)^2 \quad (22)$$

3. Pick a feasible first-stage solution $\tilde{\mathbf{X}} \in \mathbf{X}$ obtained from **Step 1** of the SAA algorithm, i.e., one of the solutions from $\hat{\mathbf{X}}_N^m$ and estimate the objective function value of the original problem [EVP] using a reference sample N' as follows:

$$\tilde{\mathbf{g}}_{N'}(\tilde{\mathbf{X}}) := \sum_{(i,j) \in (\mathcal{I}, \mathcal{J})} \sum_{t \in \mathcal{T}} m_{ijt} \tilde{X}_{ijt} + \frac{1}{N'} \sum_{n=1}^{N'} Q(\mathbf{X}, n) \quad (23)$$

The estimator $\tilde{\mathbf{g}}_{N'}(\tilde{\mathbf{X}})$ serves as a lower bound for the optimal objective function value of problem [EVP] which will be updated in each iteration if the value obtained is less than the value of the previous iteration. We now generate a large set of power demand scenarios (N') i.e., $\{\mathbf{d}^1(\omega), \mathbf{d}^2(\omega), \dots, \mathbf{d}^{N'}(\omega)\}$, $\forall n = 1, \dots, N'$. Typically, sample size N' is chosen much larger than the sample size N in the SAA problems i.e., $N' \gg N$. We can estimate the variance of $\tilde{\mathbf{g}}_{N'}(\tilde{\mathbf{X}})$ as follows:

$$\sigma_{\tilde{\mathbf{g}}_{N'}(\tilde{\mathbf{X}})}^2 = \frac{1}{(N'-1)N'} \sum_{n=1}^{N'} \left\{ \sum_{(i,j) \in (\mathcal{I}, \mathcal{J})} \sum_{t \in \mathcal{T}} m_{ijt} \tilde{X}_{ijt} + Q(\mathbf{X}, n) - \tilde{\mathbf{g}}_{N'}(\tilde{\mathbf{X}}) \right\}^2$$

4. Compute the optimality gap ($gap_{N,M,N'}(\tilde{\mathbf{X}})$) and its variance (σ_{gap}^2) using the estimators calculated in **Steps 2** and **3**.

$$gap_{N,M,N'}(\tilde{\mathbf{X}}) = \bar{\mathbf{v}}_M^N - \tilde{\mathbf{g}}_{N'}(\tilde{\mathbf{X}})$$

$$\sigma_{gap}^2 = \sigma_{\tilde{\mathbf{g}}_{N'}(\tilde{\mathbf{X}})}^2 + \sigma_{\bar{\mathbf{v}}_M^N}^2$$

The confidence interval for the optimality gap is then calculated as follows:

$$\bar{\mathbf{v}}_M^N - \tilde{\mathbf{g}}_{N'}(\tilde{\mathbf{X}}) + z_\alpha \left\{ \sigma_{\tilde{\mathbf{g}}_{N'}(\tilde{\mathbf{X}})}^2 + \sigma_{\bar{\mathbf{v}}_M^N}^2 \right\}^{1/2}$$

with $z_\alpha := \Phi^{-1}(1 - \alpha)$, where $\Phi(z)$ is the cumulative distribution function of the standard normal distribution.

5.3 Progressive hedging algorithm

Step 1 in the Sample Average Approximation algorithm requires solving a two-stage stochastic mixed-integer linear programming model with $|N|$ scenarios. Depending on the size of $|\mathcal{I}|$, $|\mathcal{J}|$, and $|\mathcal{T}|$, solving this problem can still be considered challenging. To overcome this issue, we solve each subproblem of the SAA problem using a Progressive Hedging Algorithm (PHA) (Rockafellar and Wets, 1991). The PHA proceeds by applying a scenario decomposition technique based on the augmented Lagrangian relaxation scheme to solve a number of individual scenario subproblems and finally aggregating the individual scenario solutions. The Progressive hedging algorithm has been successfully applied in a variety of different application areas, such as financial planning (Mulvey and Vladimirov, 1991), fisheries management (Helgason and Wallace, 1991), surgery planning (Gul et al., 2015), hydrothermal operation planning (Santos et al., 2009; Carpentier et al., 2013), and others. Interested readers can review the studies of Wallace and Helgason (1991), Watson and Woodruff (2011), Crainic et al. (Gabriel Crainic et al., 2016), and Manerba and Perboli (ManerbaGuido, 2019) for a detailed discussion about the algorithmic implementation.

Constraints (10) and (14) in [EVP] link the first-stage decisions with the second-stage decision variables. These constraints do not allow problem (20) to be separable by scenario. To remedy this problem, we define a new variable $\{X_{ijt}^n\}_{\forall (i,j) \in (\mathcal{I}, \mathcal{J}), t \in \mathcal{T}, n \in N'} \in \{0,1\}$ that ensures a copy of the first-stage decision variable is created for each scenario $n \in N$. Problem (20) can now be rewritten as follows:

$$\text{Maximize}_{\mathbf{X}, \mathbf{Y}, \mathbf{Z}, \mathbf{P}} \frac{1}{N} \sum_{n=1}^N \sum_{(i,j) \in (\mathcal{I}, \mathcal{J})} \sum_{t \in \mathcal{T}} \left\{ m_{ijt} X_{ijt}^n + \sum_{\substack{(k,l) \in (\mathcal{I}_i, \mathcal{J}_j) \\ (k,l) \neq (i,j)}} (\psi_{ijklt} - c_{ijklt}^r) Y_{ijklt}^n \right\}$$

subject to: (7)–(9), (11)–(13), (15)–(17), and

$$\sum_{(i,j) \in (\mathcal{I}, \mathcal{J})} c_{ijt} X_{ijt}^n \leq B_t^e \quad \forall t \in \mathcal{T}, n \in N \quad (24)$$

$$\sum_{k=i-1}^{i+1} \sum_{l=j-1}^{j+1} X_{klt}^n \leq 1 \quad \forall (i,j) \in (\mathcal{I}, \mathcal{J}), t \in \mathcal{T}, n \in N \quad (25)$$

$$X_{ijt-1}^n \leq X_{ijt}^n \quad \forall (i,j) \in (\mathcal{I}, \mathcal{J}), t \in \mathcal{T}, n \in N \quad (26)$$

$$\frac{d_{ijt}^n X_{ijt}^n}{c_{ijs}} \geq \gamma_{ijt} Z_{ijst}^n \quad \forall (i,j) \in (\mathcal{I}, \mathcal{J}), s \in \mathcal{S}, t \in \mathcal{T}, n \in N \quad (27)$$

$$\max\{d_{ijt}^n - \beta \alpha_i f_{ijt}, 0\} X_{ijt}^n \geq \sum_{k=i-1, k \neq i}^{i+1} \sum_{l=j-1, l \neq j}^{j+1} Y_{ijklt}^n \quad \forall (i,j) \in (\mathcal{I}, \mathcal{J}), t \in \mathcal{T}, n \in N \quad (28)$$

$$X_{ijt}^n = X_{ijt}^m \quad \forall n, m \in N, n \neq m \quad (29)$$

$$X_{ijt}^n \in \{0,1\} \quad \forall (i,j) \in (\mathcal{I}, \mathcal{J}), t \in \mathcal{T}, n \in N \quad (30)$$

Constraints (29) are referred to as *nonanticipativity* constraints which link the first and second-stage decision variables and force all the scenarios to yield the same value for each first-stage decision variable. This makes the model not separable by scenarios. To make the model separable by scenarios and apply Lagrangian relaxation, we need to rewrite the *nonanticipativity* constraints. Let $\{\bar{X}_{ijt}^n\}_{\forall (i,j) \in (\mathcal{I}, \mathcal{J}), t \in \mathcal{T}} \in \{0,1\}$ be the “overall design vector”. The following constraints are equivalent to (29):

$$X_{ijt}^n = \bar{X}_{ijt} \quad \forall (i,j) \in (\mathcal{I}, \mathcal{J}), t \in \mathcal{T}, n \in N \quad (31)$$

$$\bar{X}_{ijt} \in \{0,1\} \quad \forall (i,j) \in (\mathcal{I}, \mathcal{J}), t \in \mathcal{T}. \quad (32)$$

Following the decomposition technique proposed by [Rockafellar and Wets \(1991\)](#), we relax constraints (31) using an augmented Lagrangian strategy and obtain the following objective function:

$$\text{Maximize}_{\mathbf{X}, \mathbf{Y}, \mathbf{Z}, \mathbf{P}} \frac{1}{N} \sum_{n=1}^N \sum_{(i,j) \in (\mathcal{I}, \mathcal{J})} \sum_{t \in \mathcal{T}} \left\{ m_{ijt} X_{ijt}^n + \sum_{\substack{(k,l) \in (\mathcal{I}_i, \mathcal{J}_j) \\ (k,l) \neq (i,j)}} (\psi_{ijklt} - c_{ijklt}^r) Y_{ijklt}^n + \lambda_{ijt}^n (X_{ijt}^n - \bar{X}_{ijt}) + \frac{1}{2} \varphi (X_{ijt}^n - \bar{X}_{ijt})^2 \right\}$$

where $\{\lambda_{ijt}^n\}_{\forall (i,j) \in (\mathcal{I}, \mathcal{J}), t \in \mathcal{T}, n \in N}$ define the Lagrangian multipliers for the relaxed constraints and φ defines a penalty ratio. Given the binary requirements of variables $\{X_{ijt}^n\}_{\forall (i,j) \in (\mathcal{I}, \mathcal{J}), t \in \mathcal{T}, n \in N}$ and $\{\bar{X}_{ijt}^n\}_{\forall (i,j) \in (\mathcal{I}, \mathcal{J}), t \in \mathcal{T}}$ the quadratic term $\sum_{(i,j) \in (\mathcal{I}, \mathcal{J})} \sum_{t \in \mathcal{T}} \varphi (X_{ijt}^n - \bar{X}_{ijt})^2$ shown in the above objective function can be reduced as follows:

$$\begin{aligned} \sum_{(i,j) \in (\mathcal{I}, \mathcal{J})} \sum_{t \in \mathcal{T}} \varphi (X_{ijt}^n - \bar{X}_{ijt})^2 &= \sum_{(i,j) \in (\mathcal{I}, \mathcal{J})} \sum_{t \in \mathcal{T}} (\varphi (X_{ijt}^n)^2 - 2\varphi X_{ijt}^n \bar{X}_{ijt} + \varphi (\bar{X}_{ijt})^2) \\ &= \sum_{(i,j) \in (\mathcal{I}, \mathcal{J})} \sum_{t \in \mathcal{T}} (\varphi X_{ijt}^n - 2\varphi X_{ijt}^n \bar{X}_{ijt} + \varphi \bar{X}_{ijt}) \end{aligned}$$

The objective function can now be reduced as follows:

$$\text{Maximize}_{\mathbf{X}, \mathbf{Y}, \mathbf{Z}, \mathbf{P}} \frac{1}{N} \sum_{n=1}^N \sum_{(i,j) \in (\mathcal{I}, \mathcal{J})} \sum_{t \in \mathcal{T}} \left\{ \left(m_{ijt} + \lambda_{ijt}^n - \varphi \bar{X}_{ijt} + \frac{\varphi}{2} \right) X_{ijt}^n + \sum_{\substack{(k,l) \in (\mathcal{I}_i, \mathcal{J}_j) \\ (k,l) \neq (i,j)}} (\psi_{ijklt} - c_{ijklt}^r) Y_{ijklt}^n - \lambda_{ijt}^n \bar{X}_{ijt} + \frac{1}{2} \varphi \bar{X}_{ijt} \right\}$$

when the value of the overall plan $\{\bar{X}_{ijt}^n\}_{\forall (i,j) \in (\mathcal{I}, \mathcal{J}), t \in \mathcal{T}}$ is fixed, the last two terms of the above objective function becomes constant. This allows the subproblems to be decomposable by scenarios $n \in N$, and the overall problem can be formulated as follows:

$$[\text{EVP(PHA)}] \text{Maximize}_{\mathbf{X}, \mathbf{Y}, \mathbf{Z}, \mathbf{P}} \sum_{(i,j) \in (\mathcal{I}, \mathcal{J})} \sum_{t \in \mathcal{T}} \left\{ \left(m_{ijt} + \lambda_{ijt}^n - \varphi \bar{X}_{ijt} + \frac{\varphi}{2} \right) X_{ijt}^n + \sum_{\substack{(k,l) \in (\mathcal{I}_i, \mathcal{J}_j) \\ (k,l) \neq (i,j)}} (\psi_{ijklt} - c_{ijklt}^r) Y_{ijklt}^n \right\}$$

subject to

$$\sum_{(i,j) \in (\mathcal{I}, \mathcal{J})} c_{ijt} X_{ijt}^n \leq B_t^e \quad \forall t \in \mathcal{T} \quad (33)$$

$$\sum_{k=i-1}^{i+1} \sum_{l=j-1}^{j+1} X_{klt}^n \leq 1 \quad \forall (i,j) \in (\mathcal{I}, \mathcal{J}), t \in \mathcal{T} \quad (34)$$

$$X_{ijt-1}^n \leq X_{ijt}^n \quad \forall (i, j) \in (\mathcal{I}, \mathcal{J}), t \in \mathcal{T} \quad (35)$$

$$\sum_{(i,j) \in (\mathcal{I}, \mathcal{J})} \sum_{s \in \mathcal{S}} \phi_{st} Z_{ijst}^n \leq B_t^c \quad \forall t \in \mathcal{T} \quad (36)$$

$$\sum_{s \in \mathcal{S}} Z_{ijst}^n \leq 1 \quad \forall (i, j) \in (\mathcal{I}, \mathcal{J}), t \in \mathcal{T} \quad (37)$$

$$Z_{ijst-1}^n \leq Z_{ijst}^n \quad \forall (i, j) \in (\mathcal{I}, \mathcal{J}), s \in \mathcal{S}, t \in \mathcal{T} \quad (38)$$

$$\frac{d_{ijt}^n X_{ijt}^n}{\bar{c}_{ijs}} \geq \gamma_{ijt} Z_{ijst}^n \quad \forall (i, j) \in (\mathcal{I}, \mathcal{J}), s \in \mathcal{S}, t \in \mathcal{T} \quad (39)$$

$$\sum_{k=i-1, i \neq k}^{i+1} \sum_{l=j-1, j \neq l}^{j+1} Y_{ijkl}^n \leq P_{ijt}^n \quad \forall (i, j) \in (\mathcal{I}, \mathcal{J}), t \in \mathcal{T} \quad (40)$$

$$P_{ijt-1}^n - \sum_{k=i-1, i \neq k}^{i+1} \sum_{l=j-1, j \neq l}^{j+1} Y_{ijkl}^n = P_{ijt}^n \quad \forall (i, j) \in (\mathcal{I}, \mathcal{J}), t \in \mathcal{T} \quad (41)$$

$$P_{ijt}^n = \bar{p}_{ijt} \quad \forall (i, j) \in (\mathcal{I}, \mathcal{J}), t = 1 \quad (42)$$

$$\max\{d_{ijt}^n - \beta \alpha_t f_{ijt}, 0\} X_{ijt}^n \geq \sum_{k=i-1, i \neq k}^{i+1} \sum_{l=j-1, j \neq l}^{j+1} Y_{ijkl}^n \quad \forall (i, j) \in (\mathcal{I}, \mathcal{J}), t \in \mathcal{T} \quad (43)$$

$$X_{ijt}^n \in \{0,1\} \quad \forall (i, j) \in (\mathcal{I}, \mathcal{J}), t \in \mathcal{T} \quad (44)$$

$$Z_{ijst}^n \in \{0,1\} \quad \forall (i, j) \in (\mathcal{I}, \mathcal{J}), s \in \mathcal{S}, t \in \mathcal{T} \quad (45)$$

$$Y_{ijkl}^n \geq 0 \quad \forall (i, j) \in (\mathcal{I}, \mathcal{J}), (k, l) \in (\mathcal{I}, \mathcal{J}), t \in \mathcal{T} \quad (46)$$

$$P_{ijt}^n \geq 0 \quad \forall (i, j) \in (\mathcal{I}, \mathcal{J}), t \in \mathcal{T} \quad (47)$$

Here, $\{\lambda_{ijt}^{n,r}\}_{\forall (i,j) \in (\mathcal{I}, \mathcal{J}), t \in \mathcal{T}, n \in N}$ and φ^r denote the lagrangian multipliers and penalty parameter of the progressive hedging algorithm, respectively which are updated at each iteration r . The general idea of the basic Progressive hedging algorithm is to solve N deterministic [EVP(PHA)] problems and obtain the consensus parameter $\{\bar{X}_{ijt}^r\}_{\forall (i,j) \in (\mathcal{I}, \mathcal{J}), t \in \mathcal{T}}$. If the gap between the binary variable $X_{ijt}^{n,r}$ and the consensus parameter \bar{X}_{ijt}^r falls below a threshold value ε (i.e., $\varepsilon = 0.001$) for each $(i, j) \in (\mathcal{I}, \mathcal{J}), t \in \mathcal{T}$ then the algorithm terminates; otherwise, the value of $\lambda_{ijt}^{n,r}$ and φ^r are updated using equations (48) and (49) and the process continues.

$$\lambda_{ijt}^{n,r} \leftarrow \lambda_{ijt}^{n,r-1} + \varphi_{ijt}^{n,r-1} (X_{ijt}^{n,r} - \bar{X}_{ijt}^{r-1}) \quad \forall (i, j) \in (\mathcal{I}, \mathcal{J}), t \in \mathcal{T} \quad (48)$$

$$\varphi^r \leftarrow \alpha \varphi^{r-1} \quad (49)$$

where $\alpha > 1$ is a given constant and φ^0 is set to a fixed positive value to ensure that $\varphi^r \rightarrow \infty$ as the number of iteration r increases. Moreover, $\lambda_{ijt}^{n,0}$ is set to zero for each scenario $n \in N$. Pseudo-code of the basic progressive hedging algorithm is provided in **Algorithm 1**.

Algorithm 1

Progressive Hedging Algorithm

```

Initialize,  $r \leftarrow 1$ ,  $\varepsilon$ ,  $\{\lambda_{ijt}^{n,r}\}_{\forall (i,j) \in (\mathcal{I}, \mathcal{J}), t \in \mathcal{T}, n \in N} \leftarrow 0$ ,  $\varphi^r \leftarrow \varphi^0$ 
 $terminate \leftarrow \text{false}$ 
while ( $terminate = \text{false}$ ) do
  for  $n = 1$  to  $N$ 
    Solve [EVP(PHA)] and obtain  $\{X_{ijt}^{n,r}\}_{\forall (i,j) \in (\mathcal{I}, \mathcal{J}), t \in \mathcal{T}, n \in N}$ 
  end for
  Calculate the consensus parameter:
   $\bar{X}_{ijt}^r \leftarrow \frac{1}{N} \sum_{n=1}^N X_{ijt}^{n,r}; \forall (i, j) \in (\mathcal{I}, \mathcal{J}), t \in \mathcal{T}$ 
  if ( $r > 1$ ) then
    Update the largangian parameter:
     $\lambda_{ijt}^{n,r} \leftarrow \lambda_{ijt}^{n,r-1} + \varphi^{r-1} (X_{ijt}^{n,r} - \bar{X}_{ijt}^{r-1}); \forall (i, j) \in (\mathcal{I}, \mathcal{J}), t \in \mathcal{T}$ 
    Update the penalty parameter:
     $\varphi^r \leftarrow \alpha \varphi^{r-1}$  and  $\alpha > 1$ 
  end if
  if any termination criteria is met, then
     $terminate \leftarrow \text{true}$ 
  end if
   $r \leftarrow r + 1$ 
end while

```

Termination Criteria: The Progressive hedging algorithm terminates when one of the following conditions is satisfied:

- $\frac{1}{N} \sum_{n=1}^N \sum_{(i,j) \in (\mathcal{I}, \mathcal{J})} \sum_{t \in \mathcal{T}} |X_{ijt}^{n,r} - \bar{X}_{ijt}^r| \leq \varepsilon$; where ε is a pre-specified tolerance gap
- 10 consecutive non-improvement iterations
- Maximum iteration limit is reached (i.e., $iter^{max} = 100$)
- Maximum time limit is reached (i.e., $time^{max} = 10,800$ CPU seconds)

5.4 Enhanced progressive hedging algorithm

Our initial computational experimentation with the Progressive Hedging algorithm with a sufficiently large data set exposes its inability to converge within a reasonable amount of time. This motivates us to explore additional enhancement techniques (e.g., local and global heuristics, dynamic penalty parameter updating technique, rolling horizon heuristic) to improve the convergence and stability of the Progressive Hedging algorithm. Therefore, the following subsections will present some enhancement techniques to solve problem [EVP(PHA)] efficiently.

5.4.1 Penalty parameter updating

Prior studies such as (Chen and Fan, 2012; Huang et al., 2014) show that setting the value of φ highly impacts the quality of the solution produced by the Progressive Hedging algorithm. For instance, when the value of φ is too large then the algorithm converges fast to a suboptimal solution. On the other hand, if the value of φ is too low then the algorithm converges slowly to a near optimal solution. To overcome this challenge, we have used a method proposed by Hvattum and Lokketangen (2009) to dynamically adjust the value of φ over iterations based on comparing the convergence rate of the algorithm at iterations r and $r - 1$. Let Δ_1^r and Δ_2^r be indicators of the convergence rates in the dual space and in the primal space, respectively. Thus, the penalty value can be updated as follows:

$$\varphi^r = \begin{cases} \phi \varphi^{r-1} & \text{if } \Delta_1^r - \Delta_1^{r-1} > 0 \\ \frac{1}{\phi} \varphi^{r-1} & \text{else if } \Delta_2^r - \Delta_2^{r-1} > 0 \\ \varphi^{r-1} & \text{otherwise} \end{cases} \quad (50)$$

where:

$$\Delta_1^r = \sum_{i \in \mathcal{I}} \sum_{j \in \mathcal{J}} \sum_{t \in \mathcal{T}} \sum_{n \in N} (X_{ijt}^{n,r} - \bar{X}_{ijt}^r)^2 \quad (51)$$

$$\Delta_2^r = \sum_{i \in \mathcal{I}} \sum_{j \in \mathcal{J}} \sum_{t \in \mathcal{T}} (\bar{X}_{ijt}^r - \bar{X}_{ijt}^{r-1})^2 \quad (52)$$

and ϕ is a constant parameter which value is set to $\phi > 1$.

5.4.2 Heuristic strategies

As inspired by Crainic et al. (2011), we have used two heuristic strategies that modify the value of m_{ijt} in problem [EVP(PHA)] to further enhance the performance of the Progressive Hedging algorithm. The first one is termed *global heuristic* since this strategy adjusts the value of m_{ijt} at the end of each iteration r . On the other hand, the second one, referred to as *local heuristic*, adjusts the value of m_{ijt} within the scenario level.

Remember that problem [EVP(PHA)] can be decomposed into a series of N deterministic sub-problems. At the end of each iteration r of **Algorithm 1**, we can obtain the values of the consensus parameter $\{\bar{X}_{ijt}^r\}_{(i,j) \in (\mathcal{I}, \mathcal{J}), t \in \mathcal{T}}$ which provides an indication of how many times a cell $(i, j) \in (\mathcal{I}, \mathcal{J})$ at time period $t \in \mathcal{T}$ was selected in the previous iterations. A higher value of \bar{X}_{ijt}^r means that the cell $(i, j) \in (\mathcal{I}, \mathcal{J})$ at time period $t \in \mathcal{T}$ was selected in many of the previous iterations. Contrarily, a lower value of \bar{X}_{ijt}^r indicates that the cell $(i, j) \in (\mathcal{I}, \mathcal{J})$ at time period $t \in \mathcal{T}$ was not a favorable decision in most of the previous iterations. Let \bar{a} and \underline{a} be the two parameters that define the upper and lower threshold value. Therefore, if the value of \bar{X}_{ijt}^r is greater than the threshold value \bar{a} , then increasing the profit associated with selecting cell $(i, j) \in (\mathcal{I}, \mathcal{J})$ in time period $t \in \mathcal{T}$ will attract the subproblems to use the cell in the coming iterations. Similarly, if the value of \bar{X}_{ijt}^r is lower than the threshold value \underline{a} , then decreasing the profit associated with selecting cell $(i, j) \in (\mathcal{I}, \mathcal{J})$ in time period $t \in \mathcal{T}$ will discourage the use of this cell in the subproblems of the coming iterations. This will fix the decisions of using few cells in a given time period to either one or zero and thus will help reduce the size of the problem. The adjustment strategy is shown as follows:

$$m_{ijt}^r = \begin{cases} \delta m_{ijt}^{r-1} & \text{if } \bar{X}_{ijt}^{r-1} > \bar{a} \\ \frac{1}{\delta} m_{ijt}^{r-1} & \text{if } \bar{X}_{ijt}^{r-1} < \underline{a} \\ m_{ijt}^{r-1} & \text{Otherwise} \end{cases} \quad (53)$$

where m_{ijt}^r represents the modified expected profit from car traffic at cell $(i, j) \in (\mathcal{I}, \mathcal{J})$ in time period $t \in \mathcal{T}$ and iteration r , \underline{a} and \bar{a} are the two constant parameters whose values are set to $0 < \underline{a} < 0.3$ and $0.7 < \bar{a} < 1$; and δ is a constant parameter whose value is set to $\delta > 1$.

We can further enhance the *global heuristic* strategy by modifying the selection of m_{ijt} locally within the scenario level. This strategy is termed *local heuristic* (Crainic et al., 2011) since the modification of m_{ijt} only impacts the subproblem of the current scenario n at a particular iteration r . This strategy emphasizes modifying the profits associated with selecting cell $(i, j) \in (\mathcal{I}, \mathcal{J})$ in time period $t \in \mathcal{T}$ at scenario $n \in N$ and iteration r if the gap between $X_{ijt}^{n,r}$ and \bar{X}_{ijt}^r is sufficiently large. The local adjustment strategy applied to **Algorithm 1** is as follows:

$$m_{ijt}^{n,r} = \begin{cases} \delta m_{ijt}^r & \text{if } |X_{ijt}^{n,r-1} - \bar{X}_{ijt}^r| \geq a^{far} \text{ and } X_{ijt}^{n,r-1} = 0 \\ \frac{1}{\delta} m_{ijt}^r & \text{if } |X_{ijt}^{n,r-1} - \bar{X}_{ijt}^r| \geq a^{far} \text{ and } X_{ijt}^{n,r-1} = 1 \\ m_{ijt}^r & \text{Otherwise} \end{cases} \quad (54)$$

where $m_{ijt}^{n,r}$ represents the modified m_{ijt} of selecting a cell at location $(i, j) \in (\mathcal{I}, \mathcal{J})$ in time period $t \in \mathcal{T}$ under scenario $n \in N$ and at iteration r , a^{far} is a threshold point at which a local adjustment to the m_{ijt} of selecting a cell is applied and is set to $0.5 < a^{far} < 1$; and δ is a constant parameter whose

value is set to $\delta > 1$.

5.4.3 Rolling horizon heuristic strategy

Note that, the Progressive Hedging algorithm still requires that we solve a deterministic, multi-time period problem [EVP(PHA)] N times which is considered challenging from a solution standpoint. To alleviate this challenge, in this section we develop a *Rolling Horizon* ([RH]) heuristic to solve problem [EVP(PHA)]. This approach decomposes problem [EVP(PHA)] into a series of small subproblems where each subproblem includes a few consecutive time periods which are drawn from the overall planning horizon. The algorithm terminates when all the subproblems are investigated. Interested readers can review the works by Balasubramanian and Grossman (Balasubramanian and Grossmann, 2004), Kostina et al. (2011) and Marufuzzaman and Eksioglu (2016) to learn more about the [RH] algorithm. Pseudo-code of the [RH] algorithm is shown in Algorithm 2.

Let [EVP(PHA(r))] denote the approximate subproblem of the rolling horizon algorithm. We further define t_0^r and M^r to be the starting time period and number of time periods of subproblem r , respectively. Note that we can either set a fixed or variable size of M^r for the subproblems. For each scenario $n \in N$, the approximate subproblems [EVP(PHA(r))] are solved by setting the variables as: (i) $\{X_{ijt}^n\}_{\forall (i,j) \in (\mathcal{I}, \mathcal{J}), t \in \mathcal{T}} \in \{0,1\}$ and $\{Z_{ijst}^n\}_{\forall (i,j) \in (\mathcal{I}, \mathcal{J}), s \in \mathcal{S}, t \in \mathcal{T}} \in \mathbb{Z}^+$ for $t_0^r \leq t \leq t_0^r + M^r$, (ii) $0 \leq X_{ijt}^n \leq 1$ and $Z_{ijst}^n \in \mathbb{R}^+$ for $t > t_0^r + M^r$. Once a subproblem is solved, we fix the values of $X_{ijt}^{n,r} = X_{ijt}^{n,r-1}$; $\forall (i, j) \in (\mathcal{I}, \mathcal{J}), t \in \mathcal{T}$ and $Z_{ijst}^{n,r} = Z_{ijst}^{n,r-1}$; $\forall (i, j) \in (\mathcal{I}, \mathcal{J}), s \in \mathcal{S}, t \in \mathcal{T}$ for $t < t_0^r$ and update the step size r . The process terminates when all the subproblems [EVP(PHA(r))] are solved. Fig. 14 shows an example of using the rolling horizon approach to solve a three time period problem.

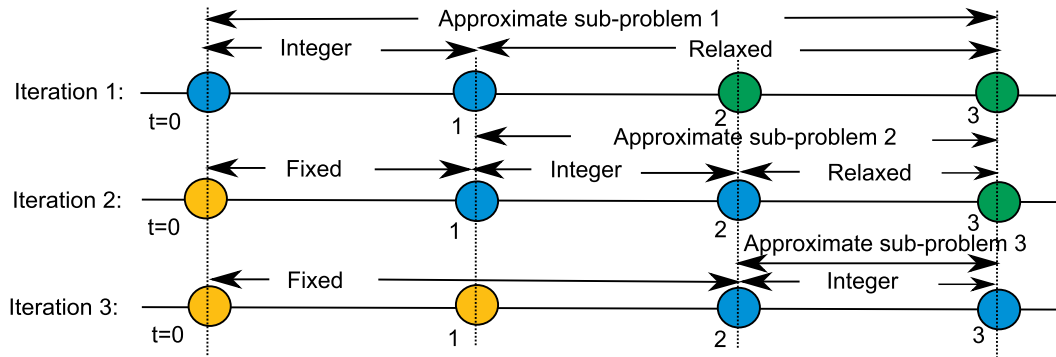


Fig. 14. Illustration of a rolling horizon strategy for a three time period.

Algorithm 2

Rolling Horizon (RH) Heuristic

```

 $r \leftarrow 1, t_0^r = 0, M^r, \text{terminate} \leftarrow \text{false}$ 
while ( $\text{terminate} = \text{false}$ ) do
  Set:
   $\{X_{ijt}^n\}_{\forall (i,j) \in (\mathcal{I}, \mathcal{J}), t \in \mathcal{T}} \in \{0,1\}$  and  $\{Z_{ijst}^n\}_{\forall (i,j) \in (\mathcal{I}, \mathcal{J}), s \in \mathcal{S}, t \in \mathcal{T}} \in \{0,1\}$  for  $t_0^r \leq t \leq t_0^r + M^r$ 
   $0 \leq \{X_{ijt}^n\}_{\forall (i,j) \in (\mathcal{I}, \mathcal{J}), t \in \mathcal{T}} \leq 1, 0 \leq \{Z_{ijst}^n\}_{\forall (i,j) \in (\mathcal{I}, \mathcal{J}), s \in \mathcal{S}, t \in \mathcal{T}} \leq 1$  for  $t > t_0^r + M^r$ 
  Solve the approximate sub-problem [EVP(PHA( $r$ ))] using CPLEX
  if ( $t_0 > |\mathcal{T}|$ ) then
     $\text{stop} \leftarrow \text{true}$ 
  else
    Fixing the values of  $\{X_{ijt}^n\}_{\forall (i,j) \in (\mathcal{I}, \mathcal{J}), t \in \mathcal{T}}, \{Z_{ijst}^n\}_{\forall (i,j) \in (\mathcal{I}, \mathcal{J}), s \in \mathcal{S}, t \in \mathcal{T}}$  for  $t < t_0^r$ 
  end if
   $\text{mile}^2$ 
end while

```

References

- Agenbrood, J., Holland, B., 2014. EV Charging Station Infrastructure Costs. Rocky Mountain Institute Available from: http://blog.rmi.org/blog_2014_04_29_pulling_back_the_veil_on_ev_charging_station_costs.
- Akhavan-Rezai, E., Shaaban, M.F., El-Saadany, E.F., Karray, F., 2015. Demand response through interactive incorporation of plug-in electric vehicles. In: 2015 IEEE Power Energy Society General Meeting, pp. 1–5.
- ArcGIS. Washington, DC. Available from: <https://www.arcgis.com/home/item.html?id=009fd190135f40e1b4678b73a6ce7ef7>.
- Balasubramanian, J., Grossmann, I., 2004. Approximation to multistage stochastic optimization in multiperiod batch plant scheduling under demand uncertainty. Ind. Eng. Chem. Res. 43 (14), 3695–3713.
- Baouche, F., Billot, R., Trigui, R., El Faouzi, N.E., 2014. Efficient allocation of electric vehicles charging stations: optimization model and application to a dense urban network. IEEE Intell. Transp. Syst. Mag. 6 (3), 33–43.
- Bayram, I.S., Michailidis, G., Devetsikiotis, M., Granelli, F., 2013. Electric power allocation in a network of fast charging stations. IEEE J. Sel. Area. Commun. 31 (7), 1235–1246.
- Carpentier, P.L., Gendreau, M., Bastin, F., 2013. Long-term management of a hydroelectric multireservoir system under uncertainty using the progressive hedging algorithm. Water Resour. Res. 49 (5), 2812–2827.
- Chang, M., Tseng, Y., Chen, J., 2007. A scenario planning approach for the flood emergency logistics preparation problem under uncertainty. Transp. Res. E Logist. Transp. Rev. 43 (6), 737–754.
- Chen, C.-W., Fan, Y., 2012. Bioethanol supply chain system planning under supply and demand uncertainties. Transp. Res. Part E 48, 150–164.
- Chen, T.D., Kockelman, K.M., 2013. The electric vehicle charging station location problem: a parking-based assignment method for Seattle. In: Transportation Research Board 92nd Annual Meeting, Washington, DC.
- Chung, S.H., Kwon, C., 2015. Multi-period planning for electric car charging station locations: a case of Korean Expressways. Eur. J. Oper. Res. 242, 677–687.
- City Light, 2010. The impact of electric vehicles on system load. Available from: https://www.seattle.gov/light/news/issues/irp/docs/dbg_538_app_d_3.pdf.
- Clean Technica, 2016. EV charging station infrastructure costs. Available from: <http://cleantechnica.com/2014/05/03/ev-charging-station-infrastructure-costs/>.
- Crainic, T.G., Fu, X., Gendreau, M., Rei, W., Wallace, S.W., 2011. Progressive hedging-based metaheuristics for stochastic network design. Networks 58, 114–124.
- Gabriel Crainic, Teodor, Gobatto, Luca, Guido, Perboli, Walter, Rei, 2016. Logistics capacity planning: a stochastic bin packing formulation and a progressive hedging meta-heuristic. Eur. J. Oper. Res. 253 (2), 404–417.

- Galus, M.D., Andersson, G., 2008. Demand management of grid connected plug-in hybrid electric vehicles (PHEV). In: IEEE Energy 2030 Conference, pp. 1–8.
- Ge, S., Feng, L., Liu, H., 2011. The planning of electric vehicle charging station based on grid partition method. In: 2011 International Conference on Electrical and Control Engineering (ICECE), pp. 2726–2730.
- General algebraic modeling system (GAMS).** Available from: <http://www.gams.com/>.
- Gul, S., Denton, B.T., Fowler, J., 2015. A multi-stage stochastic integer programming model for surgery planning. *Inf. J. Comput. In-press*.
- Guo, Z., Deride, J., Fan, Y., 2016. Infrastructure planning for fast charging stations in a competitive market. *Transp. Res. C Emerg. Technol.* 68, 215–227.
- Hajimiragha, A., Canizares, C.A., Fowler, M.W., Elkamel, A., 2010. Optimal transition to plug-in hybrid electric vehicles in Ontario, Canada, considering the electricity-grid limitations. *IEEE Trans. Ind. Electron.* 57 (2), 690–701.
- He, Y., Venkatesh, B., Guan, L., 2012. Optimal scheduling for charging and discharging of electric vehicles. *IEEE Trans. Smart Grid* 3 (3), 1095–1105.
- He, F., Wu, D., Yin, Y., Guan, Y., 2013. Optimal deployment of public charging stations for plug-in hybrid electric vehicles. *Transp. Res. Part B* 47, 87–101.
- Helgason, T., Wallace, S.W., 1991. Approximate scenario solutions in the progressive hedging algorithm. *Ann. Oper. Res.* 31, 425–444.
- Hosseini, M., MirHassani, S.A., 2015. Refueling-station location problem under uncertainty. *Transp. Res. Part E* 84, 101–116.
- Huang, Y., Fan, Y., Chen, C.-W., 2014. An integrated bio-fuel supply chain against feedstock seasonality and uncertainty. *Transp. Sci.* 48 (4), 540–554.
- Hvattum, L.M., Lokketangen, A., 2009. Using scenario trees and progressive hedging for stochastic inventory routing problems. *J. Heuristics* 15, 527–557.
- Institute for Renewable Energy, 2016. Power grid expansion and rising electricity prices Grid charges at 6-year low.** Available from: <http://www.iwr-institut.de/en/press/background-informations/182-power-grid-expansion-and-rising-electricity-prices>.
- Ip, A., Fong, S., Liu, E., 2010. Optimization for allocating BEV recharging stations in urban areas by using hierarchical clustering. In: 6th International Conference on Advanced Information Management and Service.
- Jia, L., Hu, Z., Song, Y., Luo, Z., 2012. Optimal siting and sizing of electric vehicle charging stations. In: IEEE International Electric Vehicle Conference, pp. 1–6.
- Kleywegt, A.J., Shapiro, A., Homem-De-Mello, T., 2001. The sample average approximation method for stochastic discrete optimization. *SIAM J. Optim.* 12, 479–502.
- Kostina, A.M., Guillen-Gosalbeza, G., Meleb, F.D., Bagajewicz, M.J., Jimenez, L., 2011. A novel rolling horizon strategy for the strategic planning of supply chains. Application to the sugar cane industry of Argentina. *Comput. Chem. Eng.* 35, 2540–2563.
- Kuby, M., Lim, S., 2005. The flow-refueling location problem for alternative-fuel vehicles. *Soc. Econ. Plan. Sci.* 39 (2), 125–145.
- Liu, Z., Wang, D., Jia, H., Djilali, N., Zhang, W., 2015. Aggregation and bidirectional charging power control of plug-in hybrid electric vehicles: generation system Adequacy analysis. *IEEE Trans. Sustain. Energy* 6 (2), 325–335.
- Magnanti, T.L., Wong, R.T., 1981. Accelerating Benders Decomposition: algorithmic enhancement and model selection criteria. *Oper. Res.* 29, 464–484.
- Mak, W.K., Morton, D.P., Wood, R.K., 1999. Monte Carlo bounding techniques for determining solution quality in stochastic programs. *Oper. Res. Lett.* 24, 47–56.
- Mak, H.-Y., Rong, Y., Shen, Z.M., 2013. Infrastructure planning for electric vehicles with battery swapping. *Manag. Sci.* 59, 1557–1575.
- Manerba, Daniele, Guido, Perboli, 2019. New solution approaches for the capacitated supplier selection problem with total quantity discount and activation costs under demand uncertainty. *Comput. Oper. Res.* 101, 29–42.
- Marufuzzaman, M., Eksioğlu, S.D., 2016. Designing a Reliable and Dynamic Multi-Modal Transportation Network for Biofuel Supply Chain. *Transportation Science (in press)*.
- MirHassani, S.A., Ebrazi, R., 2012. A flexible reformulation of the refueling station location problem. *Transp. Sci.* 47 (4), 617–628.
- Mulvey, J.M., Vladimirou, H., 1991. Applying the progressive hedging algorithm to stochastic generalized networks. *Ann. Oper. Res.* 31, 399–424.
- National Public Radio, 2016. The price of electricity in your state.** Available from: <http://www.npr.org/sections/money/2011/10/27/141766341/the-price-of-electricity-in-your-state>.
- Norkin, V.I., Ermoliev, Y.M., Ruszczyński, A., 1998a. On optimal allocation of indivisibles under uncertainty. *Oper. Res.* 46, 381–395.
- Norkin, V.I., Pflug, G.C., Ruszczyński, A., 1998b. A branch and bound method for stochastic global optimization. *Math. Program.* 83 (3), 425–450.
- Pan, F., Bent, R., Berscheid, A., Izraelevitz, D., 2010. Locating PHEV exchange stations in V2G. In: First IEEE International Conference on Smart Grid Communications, pp. 173–178.
- Ravichandran, A., Siroospour, S., Malysz, P., Emadi, A., 2016. A chance-constraints-based control strategy for microgrids with energy storage and integrated electric vehicles. *IEEE Trans. Smart Grid* (99), 1–14.
- Rezvani, Z., Jansson, J., Bodin, J., 2015. Advances in consumer electric vehicle adoption research: a review and research agenda. *Transp. Res. Part D* 34, 122–136.
- Frade, I., Ribeiro, A., Gonçalves, G., 2011. Optimal location of charging stations for electric vehicles in a neighborhood in Lisbon, Portugal. *Transp. Res. Rec.* 91–98 2252.
- Richardson, P., Flynn, D., Keane, A., 2012. Optimal charging of electric vehicles in low-voltage distribution systems. *IEEE Trans. Power Syst.* 27 (1), 268–279.
- Rockafellar, R.T., Wets, R.J.-B., 1991. Scenarios and policy aggregation in optimization under uncertainty. *Math. Oper. Res.* 16, 119–147.
- Rotering, N., Ilic, M., 2011. Optimal charge control of plug-in hybrid electric vehicles in deregulated electricity markets. *IEEE Trans. Power Syst.* 26 (3), 1021–1029.
- Santos, M.L.L., da Silva, E.L., Finardi, E.C., Goncalves, R.E.C., 2009. Practical aspects in solving the medium-term operation planning problem of hydrothermal power systems by using the progressive hedging method. *Int. J. Electr. Power Energy Syst.* 31, 546–552.
- Santoso, T., Ahmed, S., Goetschalckx, M., Shapiro, A., 2005. A stochastic programming approach for supply chain network design under uncertainty. *Eur. J. Oper. Res.* 167, 96–115.
- Schutz, P., Tomasgard, A., Ahmed, S., 2009. Supply chain design under uncertainty using sample average approximation and dual decomposition. *Eur. J. Oper. Res.* 409–419 199.
- Sundstroem, O., Binding, C., 2012. Flexible charging optimization for electric vehicles considering distribution grid constraints. *IEEE Trans. Smart Grid* 3 (1), 26–37.
- Sweda, T., Klabjan, D., 2011. An agent-based decision support system for electric vehicle charging infrastructure deployment. In: IEEE Vehicle Power and Propulsion Conference, pp. 1–5.
- Tesla. Model S.** Available from: <https://www.teslamotors.com/models>.
- Tong, L. Yu Z., Li, S., 2016. Market dynamics and indirect network effects in electric vehicle diffusion. *Transp. Res. D Transp. Environ.* 47, 336–356.
- U.S. Department of Energy, 2014. EV Everywhere Grand challenge road to success.** Available from: http://energy.gov/sites/prod/files/2014/02/18/eveverywhere_road_to_success.pdf.
- Verweij, B., Ahmed, S., Kleywegt, A.J., Nemhauser, G., Shapiro, A., 2003. The sample average approximation method applied to stochastic routing problems: a computational study. *Comput. Optim. Appl.* 24, 289–333.
- Wallace, S.W., Helgason, T., 1991. Structural properties of the progressive hedging algorithm. *Ann. Oper. Res.* 31, 445–456.
- Wang, Y.W., Lin, C.C., 2009. Locating road-vehicle refueling stations. *Transp. Res. Part E* 45 (5), 821–829.
- Wang, Y.W., Lin, C.C., 2013. Locating multiple types of recharging stations for battery-powered electric vehicle transport. *Transp. Res. Part E* 58, 76–87.
- Wang, H., Huang, Q., Zhang, C., Xia, A., 2010. A novel approach for the layout of electric vehicle charging station. In: International Conference on Apperceiving Computing and Intelligence Analysis, pp. 64–70.
- Washington State Department of Transportation, 2015. Washington state electric vehicle action plan.** Available from: <http://www.wsdot.wa.gov/NR/rdonlyres/28559EF4-CD9D-4CFA-9886-105A30FD58C4/0/WAEVActionPlan2014.pdf>.
- Watson, J.P., Woodruff, D.L., 2011. Progressive hedging innovations for a class of stochastic mixed-integer resource allocation problems. *Comput. Manag. Sci.* 8, 355–370.
- Xi, X., Sioshansi, R., Marano, V., 2013. Simulation-optimization model for location of a public electric vehicle charging infrastructure. *Transp. Res. Part D* 60–69 22.
- Yunus, K., De La Parra, H.Z., Reza, M., 2011. Distribution grid impact of Plug-In Electric Vehicles charging at fast charging stations using stochastic charging model. In: Proceedings of the 2011-14th European Conference on Power Electronics and Applications.
- Zhu, Z., Lambbotharan, S., Chin, W.H., Fan, Z., 2014. A stochastic optimization approach to aggregated electric vehicles charging in smart grids. 2014 IEEE Innovative Smart Grid Technologies - Asia (ISGT ASIA). pp. 51–56.